A STUDY OF THE RELATIONSHIP BETWEEN SOLAR ACTIVITIES AND EARTHQUAKES

INDRIANI SUKMA

FACULTY OF SCIENCE
UNIVERSITY OF MALAYA
KUALA LUMPUR

2017

A STUDY OF THE RELATIONSHIP BETWEEN SOLAR ACTIVITIES AND EARTHQUAKES

INDRIANI SUKMA

DISSERTATION SUBMITTED IN FULFILMENT OF THE REQUIREMENTS FOR THE DEGREE OF MASTER OF SCIENCE

DEPARTMENT OF PHYSICS
FACULTY OF SCIENCE
UNIVERSITY OF MALAYA
KUALA LUMPUR

2017

UNIVERSITY OF MALAYA

ORIGINAL LITERARY WORK DECLARATION

Name of Candidate: **INDRIANI SUKMA**

Matric No: **SGR130044**

Name of Degree: **MASTER OF SCIENCE**

Title of Project Paper/Research Report/Dissertation/Thesis ("this Work"):

A STUDY OF THE RELATIONSHIP BETWEEN SOLAR ACTIVITIES AND EARTHQUAKES

Field of Study: **SOLAR ASTRONOMY AND GEOPHYSICS**

I do solemnly and sincerely declare that:

(1) I am the sole author/writer of this Work;
(2) This Work is original;
(3) Any use of any work in which copyright exists was done by way of fair dealing and for permitted purposes and any excerpt or extract from, or reference to or reproduction of any copyright work has been disclosed expressly and sufficiently and the title of the Work and its authorship have been acknowledged in this Work;
(4) I do not have any actual knowledge nor do I ought reasonably to know that the making of this work constitutes an infringement of any copyright work;
(5) I hereby assign all and every rights in the copyright to this Work to the University of Malaya ("UM"), who henceforth shall be owner of the copyright in this Work and that any reproduction or use in any form or by any means whatsoever is prohibited without the written consent of UM having been first had and obtained;
(6) I am fully aware that if in the course of making this Work I have infringed any copyright whether intentionally or otherwise, I may be subject to legal action or any other action as may be determined by UM.

Candidate's Signature Date:

Subscribed and solemnly declared before,

Witness's Signature Date:

Name:

Designation:

ABSTRACT

The Sun is a prime source of energy while the Earth is the third planet near to the Sun and the only planet that has very large seismic activity. The solar wind interacts with the ionospheric currents and affects the Earth magnetic field causing a geomagnetic storm. Therefore, the study on the correlation between solar activity and earthquake is very important. The geomagnetic storm index was used as a mediator for this study. The observation covers from the year 1901 up to 2015 (i.e. between the 14^{th} and the middle of the 24^{th} solar cycles) for an area that covers the majority of China and its bordering countries. Data for solar activities such as sunspot number and solar wind parameters, including the speed, dynamic pressure and input energy of solar wind, were collected from Solar Influences Data Analysis Center (SIDC) and Advanced Composition Explorer (ACE), respectively. Data for geomagnetic storm indices such as disturbance storm time (DST) index, 3-h planetary index (Kp) and an average of the planetary index (Ap) were obtained from the National Aeronautics and Space Administration (NASA) via OmniWeb Data Explorer and the Space Physics Data Facility. Data number of the earthquake for the small ($M<4.9$) and large ($M>4.9$) magnitude in Richter scale were obtained from U.S geological survey database (USGS). The analysis focused on the variation in the number of earthquakes by considering solar wind and geomagnetic storm index based on the ascending and descending phases of each solar cycle. It is found that the number of earthquake occurrences increases during the descending phases of the solar cycle. It is predicted that there will be significantly more number of earthquakes within the next 3 years until 2019.

ABSTRAK

Matahari adalah sumber utama tenaga, manakala Bumi adalah planet ketiga berhampiran dengan Matahari dan satu-satunya planet yang mempunyai aktiviti seismik yang sangat besar. Angin suria berinteraksi dengan arus ionosfera dan memberi kesan kepada medan magnet Bumi yang menyebabkan ribut geomagnetik. Oleh itu, kajian mengenai hubung kait antara aktiviti solar dan gempa bumi adalah sangat penting. Indeks ribut geomagnetik telah digunakan sebagai pengantara untuk kajian ini. Pemerhatian meliputi dari tahun 1901 sehingga 2015 (iaitu di antara kitaran suria yang ke 14 dan pertengahan ke 24) bagi kawasan yang meliputi sebagian besar China dan negara-negara yang bersempadan. Data untuk aktiviti suria seperti nombor tompok pada matahari dan parameter angin suria, termasuk kelajuan, tekanan dinamik dan tenaga input angin suria, dikumpulkan dari tapak web Solar Influences Data Analysis Center (SIDC) and Advanced Composition Explorer (ACE), masing-masing. Data untuk indeks ribut geomagnetik seperti masa indeks gangguan ribut (DST), 3-jam Indeks planet (Kp) dan purata indeks planet (Ap) telah diperolehi daripada National Aeronautics and Space Administration (NASA) melalui tapak web OmniWeb Data Explorer dan Space Physics Data Facility. Data nombor gempa bumi untuk magnitude kecil ($M < 4.9$) dan besar ($M > 4.9$) dalam skala Richter telah diperolehi dari pangkalan data U.S Geology Survey (USGS). Analisis ini ditumpukan kepada variasi dalam bilangan gempa bumi dengan mempertimbangkan angin suria dan indeks ribut geomagnetik berdasarkan fasa menaik dan menurun setiap kitaran suria. Ia didapati bahawa bilangan kejadian gempa bumi meningkat semasa fasa menurun kitaran suria. Adalah dijangkakan bahawa akan ada lebih ketara bilangan gempa bumi dalam tempoh 3 tahun akan datang sehingga 2019.

ACKNOWLEDGEMENTS

First at all, I would like to acknowledge my supervisor, Associate Professor Dr. Zamri Zainal Abidin for his advice and beneficial discussion for without him I would not have completed my master studies. This project is indebted to Dr. Bijan Nikouravan for his idea, advice, and sharing of knowledge. I would also like to give my appreciation to Dr. Mohamad Huzaimy Jusoh from Universiti Teknology MARA (Malaysia), for sharing his knowledge and solar wind parameters archives database website. I would like to thank all the lab members of the Radio Cosmology Laboratory, especially Prof. Dr. Zainol Abidin Ibrahim for sharing their literature. Last but not least, an honorable thank you to my family; my father (Sukardi SPd), my mother (Marianis S.Pd), my sisters; Fitriani Sukma Amkeb and Nurbaiti Sukma S.Pd, my brother in low (Juarlis), and the beautiful niece Putri Mutiara for their support and prayers.

TABLE OF CONTENTS

LIST OF FIGURES

LIST OF TABLES

LIST OF SYMBOLS AND ABBREVIATIONS

Ap	:	Average planetary index
CSC	:	Conventional Solar Cycle
CIR	:	Corotating interaction region
CME	:	Coronal mass ejection
DST	:	Disturbance storm time
EQ	:	Earthquake
Kp	:	3-hour interplanetary index
MSC	:	Modified Solar Cycle
SWS	:	Solar Wind Speed
SC	:	Solar Cycle
SW dynP	:	Solar wind dynamic pressure
SN	:	Sunspot Number
SW ε	:	Solar wind input energy

LIST OF APPENDICES

CHAPTER 1: INTRODUCTION

1.1 Research Background

Sun is the main source of energy in the solar system while the earth is the third planet nearest to the sun and It is the only planet that has a very large seismic activities (Jusoh et al., 2012). The sun is magnetically active with a period of about 11 years and it is called the solar cycle (Gnevyshev, 1967; Howard & LaBonte, 1980). The activities of the sun ae referred to as the solar activities, which include; sunspot, solar wind, corona mass ejection (CME), corotating interaction region (CIR) from corona hole, solar flare and solar radio burst (Gnevyshev, 1967; Krüger, 2012). Several researchers, such as Akasofu and Chapman (1972), Bartels (1932), Budyko (1969) and Simpson (1967) consider these events in order to study the impact of the sun's energetic particles on various natural phenomena on earth such as; climate change, geomagnetic storm and seismic activity. However, the mechanism of the sun – earth magnetosphere layer connection, especially by considering the geomagnetic storm activities, is one of the greatest mysteries to scientists and geologists for centuries, especially in the study of their association to earthquake (Sukma & Abidin, 2017).

The solar wind interacts with earth's magnetosphere layer (earth's magnetic field) (Delamere, 2015; Kovner & Feldstein, 1973; Surkov & Hayakawa, 2014). Likewise, the earth's magnetic field interacts with the magnetic field of the lithosphere layer, which may assist us in studying the mechanism of solar activities influence on tectonic plate motion. The general concept of solar wind and magnetosphere coupling is illustrated in Figure 1.1.

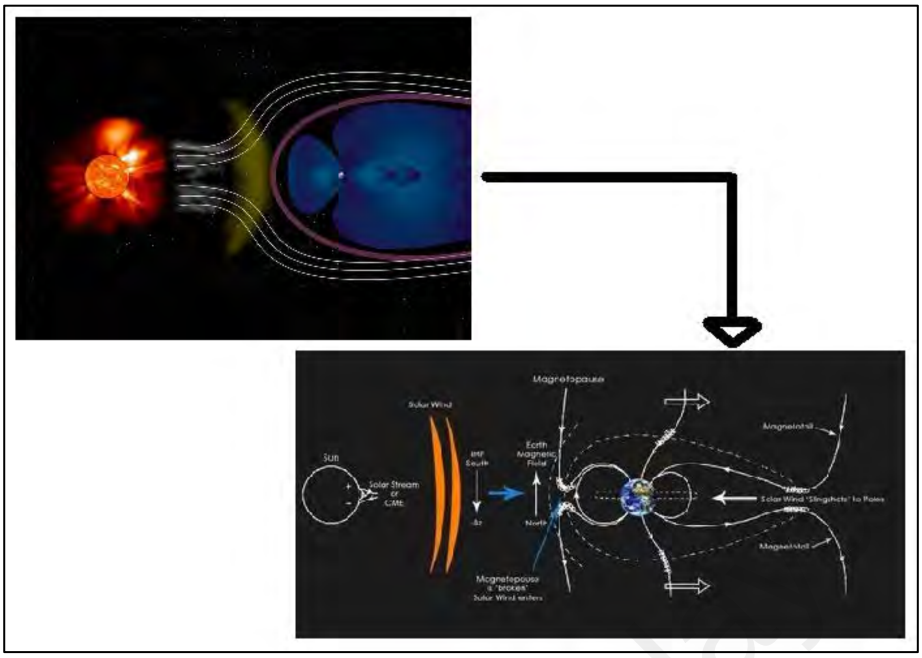

Figure 1.1: Figure of showing the interaction of solar wind energetic particles and earth magnetic field (credit: ESA).

Figure 1.1 shows the wind particles from the sun called the solar wind buffets the earth's magnetic field. Interaction between solar wind and earth's magnetic field respond to the behavior and movement of the earth's core (see Figure 1.2).

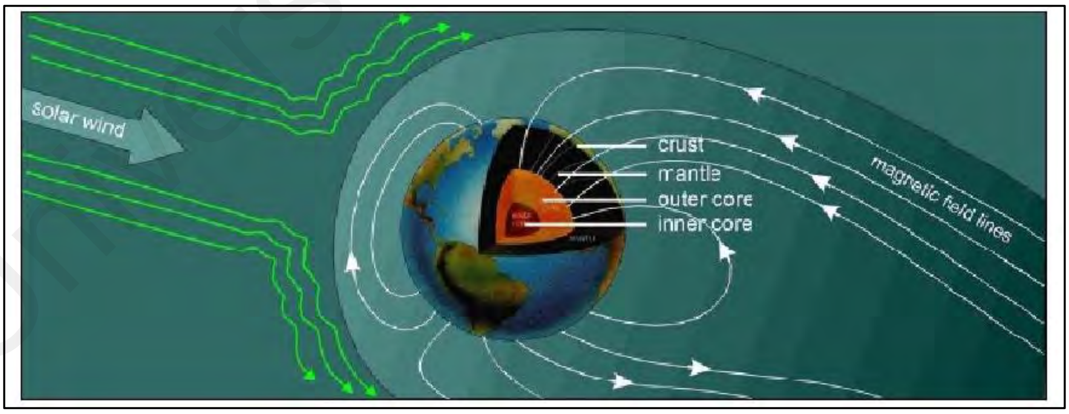

Figure 1.2: Solar wind interacting the earth's magnetic field and earth's core (Credit: DTU Space).

In order to study the solar activities, we look at the variation of sunspot number and solar wind parameters, including; speed, dynamic pressure and input energy of the solar wind. On the other hand, the geomagnetic storm indices, such as; DST, Kp and Ap were examined as physical parameters to study the solar and seismicity connection. The general concept on solar activities and geomagnetic storm coupling, and their association with earthquake activity is illustrated in Figure 1.3.

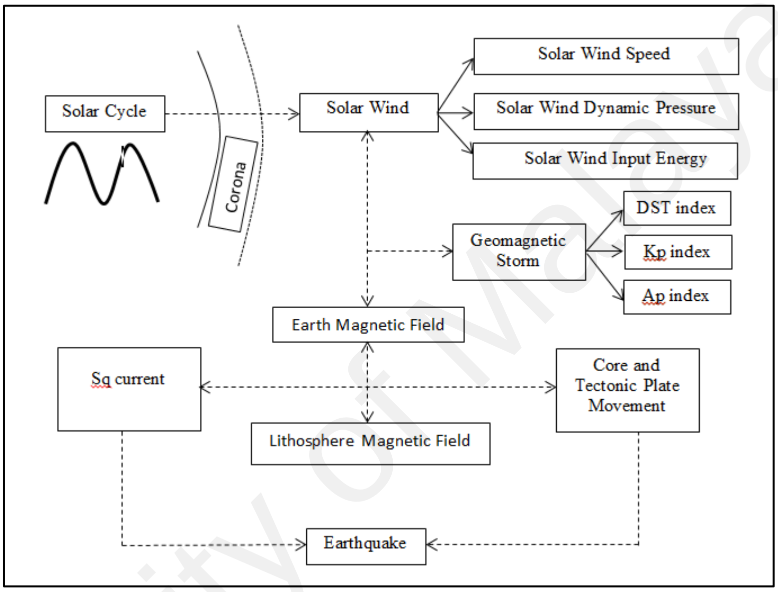

Figure 1.3: The General concept of solar and seismic activities coupling.

Basically, the frame of reference of this research focuses on the solar and seismic activity coupling by considering the concept as illustrated in Figure 1.3. Duma and Vilardo (1998) studied the relation between solar radio flux and earth's magnetic field and their association to earthquake in the local study area: Mt. Vesuvius. They found that there is correlation between them. The earth's magnetic field protects our planet from the energetic particles of the solar wind (Lang, 1995). However, there is a phenomena for which the earth magnetic field is not enough to protect the earth, namely during enhanced transfer of energetic particles of the solar wind into the magnetosphere (Gonzalez et al., 1994). Gonzalez et al. (1994) proposed that this phenomenon is called as a geomagnetic storm activity.

The classification of geomagnetic storms have been studied by Mayaud (1980). On the other hand, Biktash (2012) studied the variation of the solar wind velocity and DST index during the 19^{th} up to the 23^{rd} solar cycle. They found that, their variation had a maxima value during the descending phase in each solar cycle. Hundhausen (1979) also found the variation of solar wind to be at maxima value during descending phase. They also mentioned that the variation solar wind is dependent on variation of the activities, such as; CME (corona mass ejection) and corona interaction rotation (CIR) from corona. These events will be explained briefly in Chapter 2.

In the interaction between the solar wind and earth's magnetic field studies, several researchers had noted their association with earthquake. Anagnostopoulos and Papandreou (2012) investigated the daily variation of earthquakes with magnitude M>6.8. Their investigations showed that the occurrences of earthquake about ±1.5 days after a sudden increase in Kp index triggered by the high speed of solar wind. Sobolev et al. (2001) and Zakrzhevskaya and Sobolev (2002) also found the evidence of statistical correlation between geomagnetic storms and seismic activity. Gousheva et al. (2003) and Odintsov et al. (2006) proposed that the maximum value of earthquake in every solar cycle is found – one corresponding with solar maxima, and the other one about ±3 years after solar maxima (during the descending phase). Recently, Sukma and Abidin (2017) studied the variation of earthquakes by considering ascending and descending phases of the solar cycle. They also found that the maximum value of earthquake occurs during the descending phase. On the other hand, they only focused on solar wind speed and DST index activities as physical parameters of solar and seismic coupling. In this research, however along with dynamic and input energy of the solar wind, Kp and Ap indices are involved.

1.2 Motivation

Even though several researchers such as Duma and Vilardo (1998), Gousheva et al. (2003), Duma and Ruzhin (2003), Khain and Khalilov (2007), Rabeh et al. (2010), Anagnostopoulos and Papandreou (2012) and Midya and Gole (2014) have been studied and investigated the correlation between solar and seismic activities, but few of them concentrate on their variation by considering the ascending and descending phases in long term solar cycle variation. Basically, their research covers different phases of the solar cycles, while our research covers long term variation of solar cycles, including currently solar cycle (24^{th} solar cycle).

We are motivated to study the solar and seismic activities correlation by considering the mechanism of interaction between the solar wind and earth's magnetic field which affects the geomagnetic storm indices, likewise the earth's magnetic field interacts with the lithosphere magnetic field. Moreover, these interactions influence the induced Sq-current current (Duma & Ruzhin, 2003).

As we mentioned in the research background, the activities of the sun varies in a cycle of about 11 years. Hence, we are also motivated to study and investigate the variation of seismic activities during the ascending and descending phases of the solar cycle by considering the variation of solar wind and geomagnetic storm activities.

1.3 Research Objectives

Recently, many researchers have investigated the relationship between solar activity and earthquakes with different physical aspects, longitude and latitude study area, and the range of the solar cycle. The speed, dynamic pressure and input energy of the solar wind are treated as a physical mechanism in order to study the energy transfer in to the magnetosphere. On the other hand, the DST index, KP and Ap indices are used as a moderator in order to investigate the correlation between solar and seismic activities.

As mentioned before, the earthquake can be happen in different longitude and latitude. As shown in Figure 1.4, China is one of the countries that have large seismicity (i.e Himalaya and Vicinity). Therefore, this research is focused on the earthquakes with occurring in area that covers the majority of China and its bordering countries.

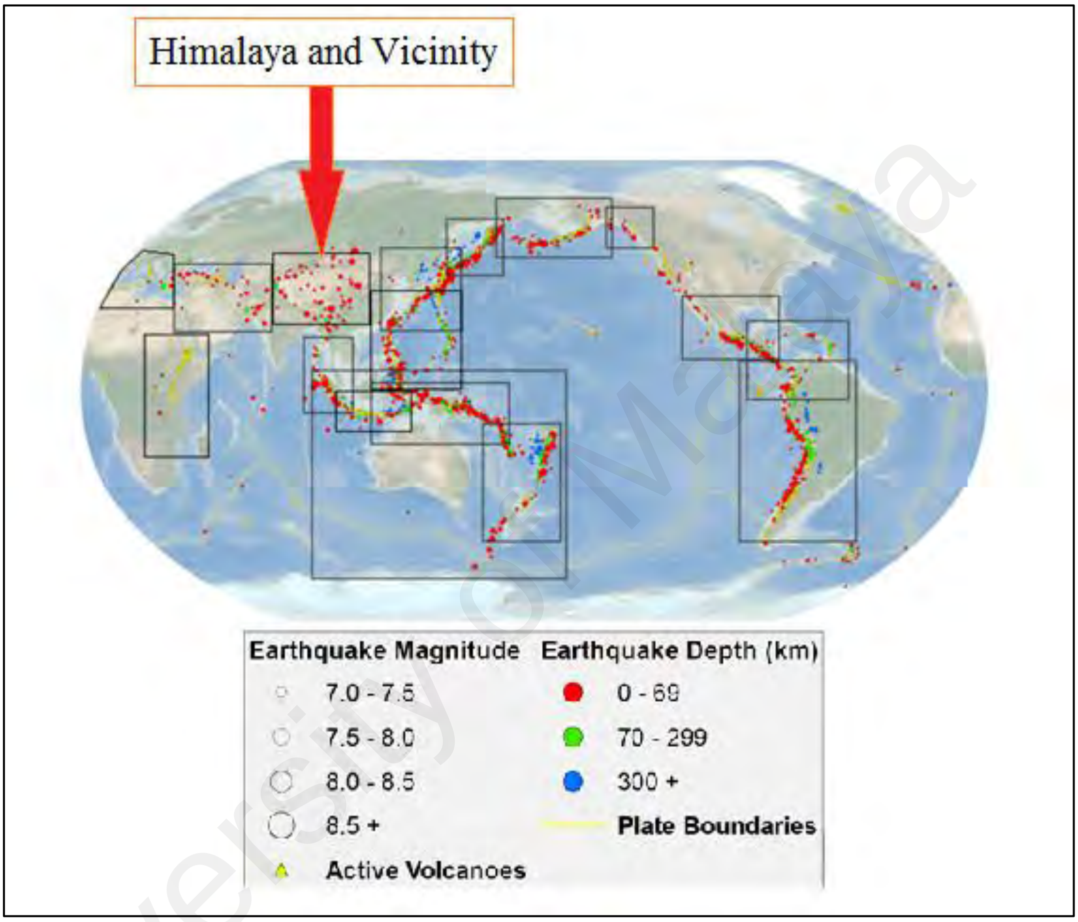

Figure 1.4: Seismicity of the global map 1900-2003 (Credit: USGS).

In general, in order to study the correlation between solar and seismic activities, this research aims;

1. To study the variation of solar wind parameters (speed, dynamic pressure and input energy of the solar wind) and geomagnetic storm indices (DST, Kp and Ap indices) during the 21st up to middle of the 24th solar cycle and investigate their maximum value in every solar cycle.
2. To study the variation of the solar wind parameters and geomagnetic storm indices by considering the ascending and descending phases of the solar cycle and investigating their correlation.
3. To evaluate the maximum value (in every solar cycle) of the annual number of small magnitude earthquakes ($M<4.9$) during the 21st up to middle of the 24th solar cycle and examine their association with solar wind and geomagnetic storm activities.
4. To evaluate the maximum value (in every solar cycle) of the annual number of large magnitude earthquakes ($M>4.9$) during the 14th up to middle of the 24th solar cycle and examine their association with the solar wind and geomagnetic storm activities.
5. To investigate the variation of small and large magnitude earthquakes by considering the ascending and descending phases of the solar cycle and explaining their association with solar wind and geomagnetic storm activities.
6. To predict the variation of small and large magnitude earthquakes during the incomplete 24th descending phase of the solar cycle.

1.4 Outline of the Research

Overall, this research is divided into six chapters. The outline of this research is structured as follows (see Table 1.1).

Table 1.1: The structure of research outline.

No. of Chapter	Title of Chapter	Explanation
1	Introduction	This chapter introduces the background of the study of solar and seismicity coupling. This chapter also provides the motivation and objectives of this research.
2	Literature Review	This chapter provides the literature review in 3 sections. Firstly, the literature review on the Sun and its activities, such as; sunspot number, corona mass ejection (CME), corotating interaction region (CIR) from corona hole and solar wind activities. The second part provides the literature review on magnetosphere and the geomagnetic storm index. Thirdly, it covers the literature review regarding Earth and its layers. From this section, the literature review on seismic activities such as earthquakes was also provided.
3	Methodology	This chapter explains the methodology on data collection. This chapter also explains the database centers that were used in this research.
4	Results and Analysis	This chapter presents and analyses the data of sunspot number, solar wind parameters (speed, dynamic pressure and input energy of the solar wind), geomagnetic storm indices (DST, Kp and Ap indices) and earthquake for small ($M<4.9$) and large ($M>4.9$) magnitude. This chapter also presents data prediction and analysis in order to predict the earthquakes
5	Discussion	This chapter discusses the possible physical mechanism on studying the correlation between solar and seismic activities. This chapter also discusses the result from Chapter 4.
6	Conclusion and Future Work	The summary of this research and discusses ideas for future work are presented in this chapter.

CHAPTER 2: LITERATURE REVIEW

2.1 Sun

At about the rate of 3.85×10^{24} joule/year, the sun radiates energy directed towards the earth (Smil, 2012; Whiteman, 2000). Basically, the sun is divided into two regions, namely; the solar interior and solar exterior (see Figure 2.1).

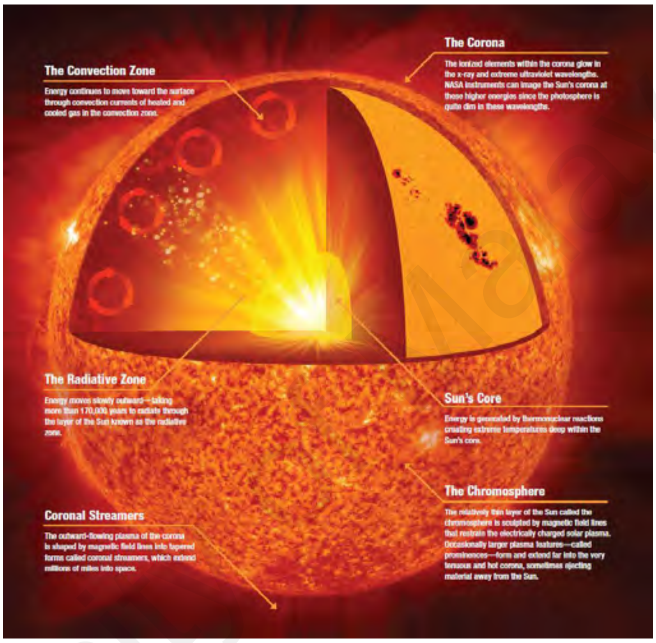

Figure 2.1: The structure of the solar interior and the solar exterior regions (Credit: NASA).

By referring to Figure 2.1, the solar interior region consists of three layers; which are core, radiative and convection zones. There is a transition layer between the radiation and convection zones, called the tachocline zone (Lang, 2002; Spiegel & Zahn, 1992). Charbonneau et al. (1999), Dalsgaard and Thompson (2007) and Elliott and Gough (1999) proposed that the thickness of tachocline zone is about less than 5% of the solar radius. On the other hand, this region is suitable for the study of the solar dynamo process (Miesch, 2005; Stenflo & Kosovichev, 2012).

In general, the solar exterior consists of two layers; the chromosphere and corona (see Figure 2.1). The interface layer between them is called the transition region. Watson (2012) mentions that the transition region has large temperature gradient. He also mentions that it is only few thousand kilometers thick with the temperature increasing from thousands to millions of Kelvin. The layers in the solar exterior have its own characteristics and different physical properties. The schematic properties of the temperature and mass density in the solar photosphere, chromosphere, corona and transition region are illustrated in Figure 2.2.

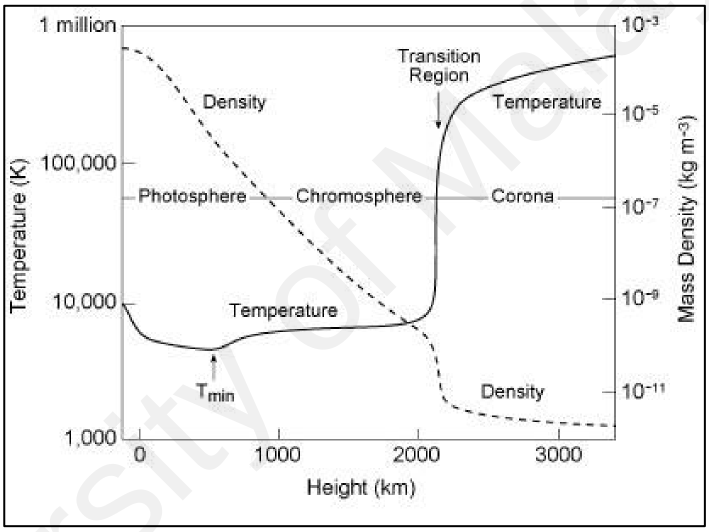

Figure 2.2: The schematic diagram of temperature (solid curve) and gas mass density (dashed curve) in the solar photosphere, chromosphere, corona and transition region. This plot credit to Praderie et al. (1981).

2.1.1 Solar Activity

The solar activity is affected by a crucial of dynamic magnetic field of the sun (Watson, 2012). The term solar activity refer to the sunspot, corotating interaction region (CIR) from corona layer, coronal mass ejection, and solar wind, including the speed, dynamic pressure and input energy of the solar wind.

2.1.1.1 Sunspot

Basically, the sunspot is a dark spot appear in the photosphere layer (Chitre, 1963; Deinzer, 1965; Thomas & Weiss, 1992). The darkness at the central region as illustrated in Figure 2.3 is caused by their strong magnetic field which affects the cooler temperature on that dark region called umbra region, which is surrounded by brighter region (penumbra region) (Brandt et al., 1990; Brummell et al., 2008; Lites & Thomas, 1985; Thomas & Weiss, 1992).

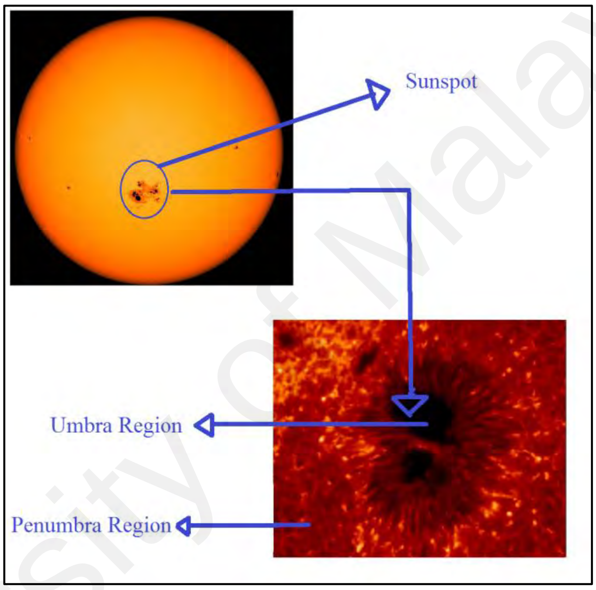

Figure 2.3: The image of sunspot activity (Credit: NASA).

In addition, the sunspot number is used in order the measure the sunspot activity. It is the oldest and longest measure of the sun's activity. The sunspot number is calculated by normalization constant (*k*), the group sunspot number (*g*) and the total sunspot number (*f*) (Brekke, 2012; Hoyt & Schatten, 1998; Waldmeier, 1961) (see Equation (1)).

$$R = K(10g + f) \tag{1}$$

On the other hand, the variation of sunspot number is well known to the study of the solar activity over an 11 year cycle (solar cycle). In this research we assumed the variation of sunspot number as the conventional solar cycle. Moreover, every solar cycle consists of 4 phases; minima, ascending, maxima and descending. These phases in one solar cycle are illustrated in Figure 2.4, while the data was retrieved from SIDC. Other than sunspot number, the variation of the solar cycle during the ascending and descending phases can also be measured by various activities of the sun, such as solar radio flux (Song et al., 2005), solar extreme ultraviolet (Solomon et al., 2010), solar flare (Gupta & Basu, 1965), cosmic ray (O'Brien, 2007), and solar wind (Gosling & Bame, 1972; Neugebauer, 1975; Webb & Howard, 1994).

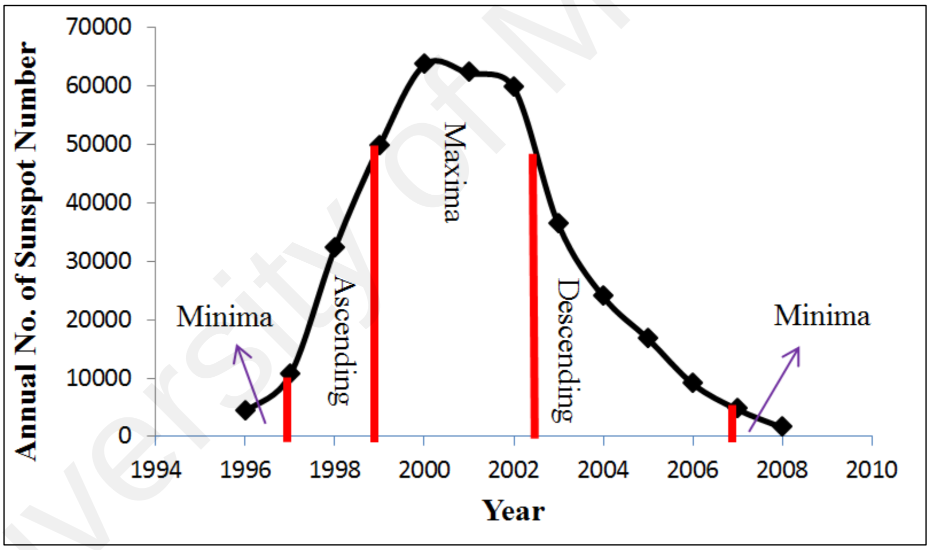

Figure 2.4: The variation of sunspot number and its phases during the 23rd solar cycle.

2.1.1.2 Coronal mass ejection

The coronal mass ejection (CME) is an explosive phenomena in the solar coronal hole layer that produces and spreads out the energy into the interplanetary medium (Benjamin & Nayar, 2010). The slow and fast coronal mass ejection interacts with the interplanetary magnetic field and the solar wind. It is divided into two categories, one is slow CME activity which accelerates and the other one is fast CME activity which decelerates towards the solar wind (Benjamin & Nayar, 2010). The study of the CME and its association with the solar wind in the solar cycle has been studied by several authors, such as Benjamin and Nayar (2010), Richardson and Cane (2012) and Richardson et al. (2000). From their study, they concluded that the explosive event of CME occur solar maxima and their variation follow the variation sunspot number in solar cycle. The illustration of CME activity is presented in Figure 2.5.

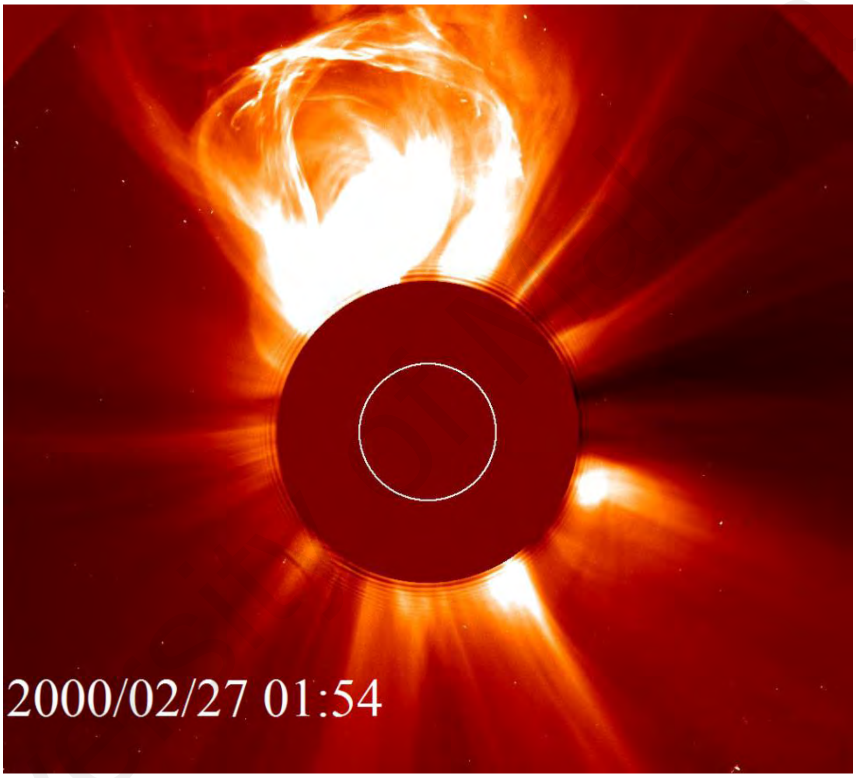

Figure 2.5: The massive of CME activity on 27 February 2000 (Credit: SOHO).

2.1.1.3 Corotating interaction region

The phenomenon of the corotating interaction region (CIR) occurs because of the solar wind interaction at different speeds and it emanates from solar corona holes region (Gosling, 1996; Prise et al., 2015; Tsurutani et al., 1995). The illustration and schematic of CIR are presented in Figure 2.6.

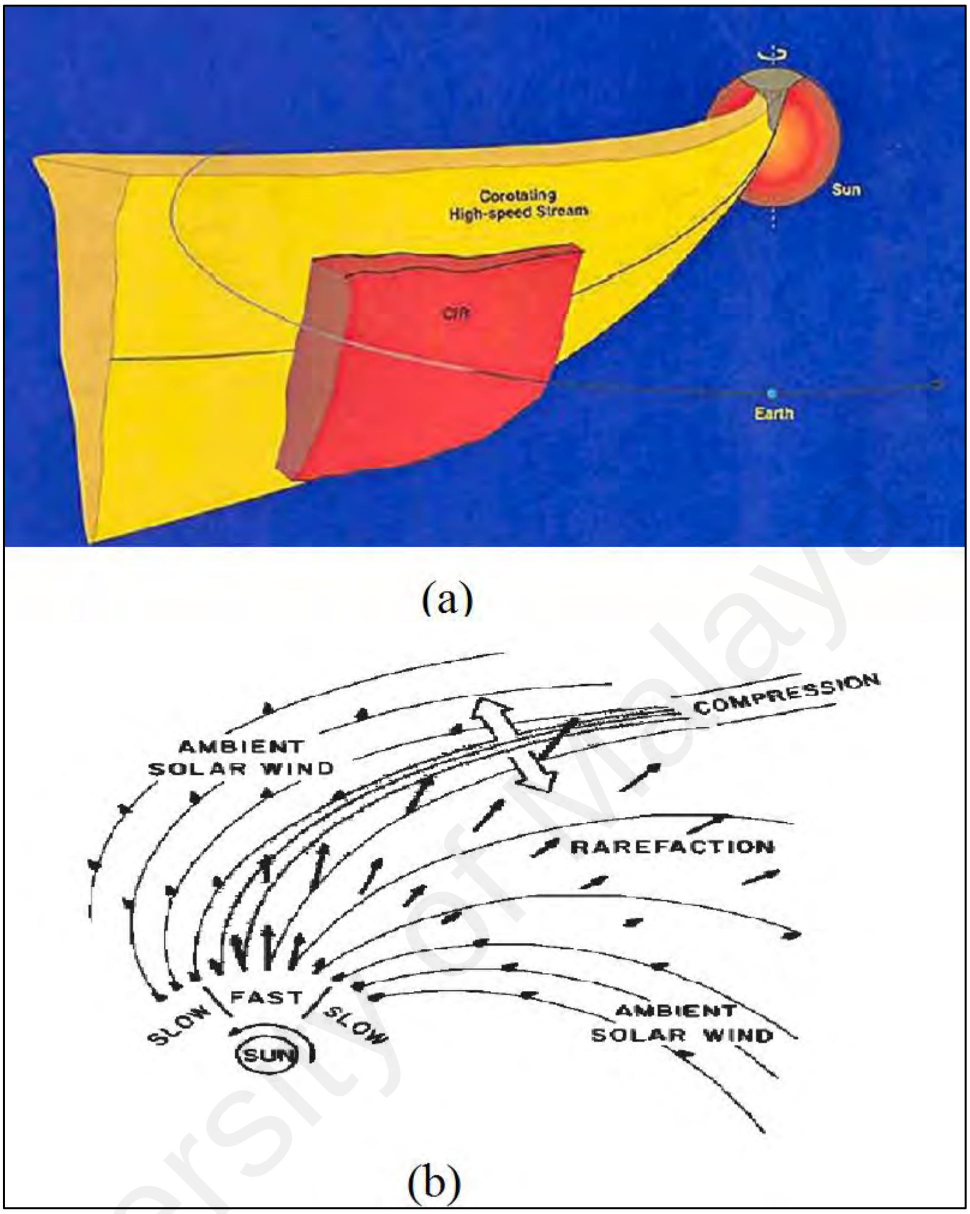

Figure 2.6: The illustration of (a) CIR activity from solar corona hole and (b) the schematics diagram of CIR (Pizzo, 1978).

The study of CIR activity, especially its explanation regarding solar wind and solar cycle have been studied by previous researchers such as Ballatore (2002), Guarnieri et al. (2006), Hundhausen (2012), Pizzo (1978), Richardson et al. (2000) and Xiao-Fei et al. (2015). From their investigation, they concluded that the CIR activity mostly occurs during the year after solar maxima which is during the descending phase of the solar cycle. During the descending and minima phases, the sun has less activity especially CME. On the other hand, during the year after solar maxima, the activity from the solar coronal hole expand in size and the energy move towards the solar equator (Guarnieri et al., 2006; Hundhausen, 2012). Therefore, the maximum of activities of the sun are not only during solar maxima, especially CIR activity which has maximum activity during descending phase.

2.1.1.4 Solar wind

The solar wind is one of the solar activities and it is the prime energy transfer and affects into and affects the magnetosphere layer. Akasofu (1981), Lu et al. (2008), Nakano et al. (2009) and Xiao-Fei et al. (2015) have studied the physical mechanism of the solar wind by considering its parameters, such as; the speed, dynamic pressure and input energy. They also investigated these parameters in association with geomagnetic storm indices by including the explanation of the CME and CIR in this study.

(a) ***Solar wind speed***

The flow of the solar wind into the interplanetary magnetic field (IMF) which affects the earth's magnetic field can be quantified by studying the speed of the solar wind. The technique of this quantification was studied by Arge et al. (2003). The solar wind speed correlates to the dynamic and input energy of the solar wind (see Equations (2) and (3)).

(b) ***Solar wind dynamic pressure***

The effects of the solar wind energy transfer into the magnetosphere and ionosphere system are known as solar wind dynamic pressure (Adebesin et al., 2013). The study of the solar wind dynamic pressure and their possible effects on the earth's magnetic field, especially in study its association to geomagnetism have been discussed by Nakano et al. (2009), Roelof and Sibeck (1993) and Xiao-Fei et al. (2015). The solar wind dynamic pressure is caused by the enhancement of the solar wind speed and proton density. On the other hand, the solar wind dynamic pressure (Pdyn) can be calculated by considering the value of solar wind speed (v) in km/s and proton density of the solar wind (np) in N/cm^3 (see Equation (2)).

$$\mathrm{SW\,Pdyn} = 1.6726\,\mathrm{e}^{-6} * nP * v^2 \left[\mathrm{nPa}\right] \tag{2}$$

(c) ***Solar wind input energy***

The penetration of solar wind input energy into the magnetosphere layer is an important process in solar physics. This input energy can be used to estimate the energy transferred by solar wind that flows into the magnetosphere and ionosphere layer (Tenfjord & Østgaard, 2013). The solar wind input energy labelled as ε have been studied by several researchers, such as Akasofu (1981) and Koskinen and Tanskanen (2002). They proposed the equation to calculate the solar wind input energy (ε) by using total magnetic field (B), clock angle (θ) and effective area of interaction (I_0) (see Equation (3)). $\left(\mu_0 \text{ is } 4\pi \times 10^{-7}\, Vs/Am\right)$.

$$\text{Epsilon}\left(\varepsilon\right) = \frac{4\pi}{\mu_0} vB^2 \sin^4\left(\frac{\theta}{2}\right) I_0^{\,2} \left[\text{Watt or Erg/s}\right] \tag{3}$$

2.2 Magnetosphere and Earth Magnetic Field

The earth has a magnetic field which is the most important shield region in order to protect our planet from energetic particles of the sun by the solar wind. This region called as magnetosphere (Hynönen, 2013; Lanza & Meloni, 2006). The illustration and of the earth's magnetosphere region is illustrated in Figure 2.7.

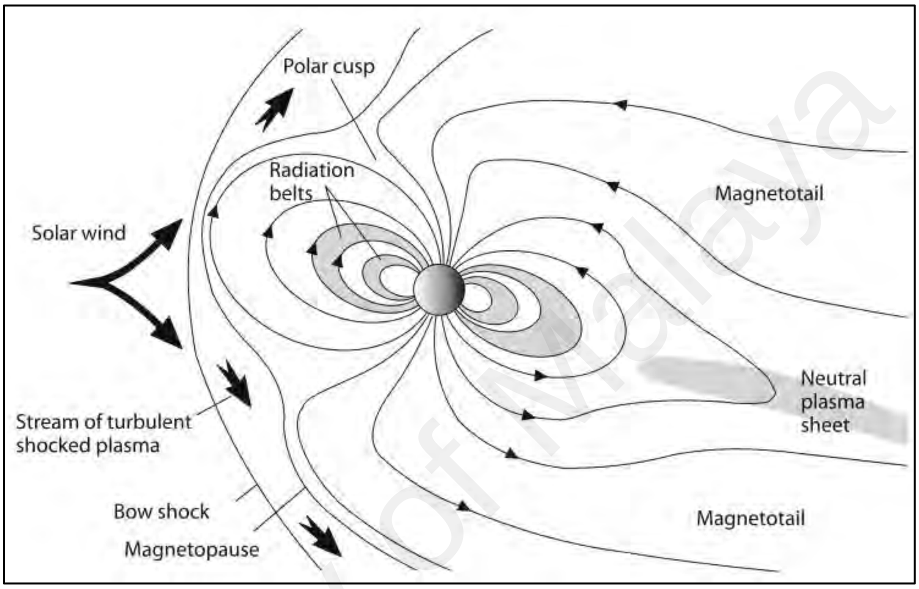

Figure 2.7: The structure of the earth's magnetosphere (Lanza & Meloni, 2006).

The shape of the magnetosphere is depending on the solar activity, especially the energetic and dynamic pressure of the solar wind. The characteristic of the boundary between solar wind and magnetosphere called as the magnetopause. Merrill and McElhinny (1983) mentioned that the bow show is formed during the period of high speed of energetic particle from solar wind collides the magnetosphere region. The magnetosphere also can be referred as an area to several fluctuation phenomena of magnetic field, such as; geomagnetic storm, auroral substorm pulsations (Hynönen, 2013).

2.2.1 Geomagnetic Storm Index

The geomagnetic storm is the phenomena to study the disturbance in the magnetosphere which is caused by the interaction between earth's magnetic field and solar wind (Gonzalez et al., 1994; Hynönen, 2013; Mayaud, 1980).

This phenomenon is measured by several indices and three of them are DST, Kp and Ap indices (Mayaud, 1980). The index of geomagnetic storm phenomena is commonly used as physical parameters on study the solar and seismicity correlation.

2.2.1.1 DST index

Gonzalez et al. (1994) mention that the daily storm time (DST) is the most common to measure and classify the geomagnetic storm index. Loewe and Prölss (1997) classified the storm based on minimum DST index (see Table 2.1)

Table 2.1: The classification of storm based on minimum DST index.

Storm Type	Minimum DST index below
Weak storm	-30 nT
Moderate storm	-50 nT
Strong storm	-100 nT
Severe storm	-200 nT
Great Storm	-350 nT

2.2.1.2 Kp and Ap indices

Kp index (3-hour planetary) is another common to measure the geomagnetic storm activity (Hynönen, 2013). The Kp index is derived from K-index planetary. Jankowski and Sucksdorff (1996) proposed the range of the K-index planetary, which is from zero to nine digits. They mentioned that the zero value of Kp index indicates as no magnetic activity while nine digit indicates as significant of geomagnetic storm activity. They also proposed the standard scale of K-index (see Table 2.2).

Table 2.2: The standard scale of K-index planetary.

K-Value	0	1	2	3	4	5	6	7	8	9
Range (nT)	0	5	10	20	40	70	120	200	300	500

The Ap index also well known as linear index, its measure by an average of 8 digits from the ap indices, where the 3-hour index ap is derived based on conversion of the quasi logarithmic 3-hour Kp index (Hynönen, 2013; Mayaud, 1980; Meyer, 2006; Rostoker, 1972). The standard conversion of Kp index correspond to the ap index were carried by Rostoker (1972) (see Table 2.3).

Table 2.3: The conversion scale amplitude from Kp to ap.

Kp (nT)	**ap (nT)**	**Kp (nT)**	**ap (nT)**
0_0	0	5_-	39
0_+	2	5_0	48
1_-	3	5_+	56
1_0	4	6_-	67
1_+	5	6_0	80
2_-	6	6_+	94
2_0	7	7_-	111
2_+	9	7_0	132
3_-	12	7_+	154
3_0	15	8_-	179
3_+	18	8_0	207
4_-	22	8_+	236
4_0	27	9_-	300
4_+	32	9_0	400

2.3 Earth Seismicity

The study of earthquake physics is a very complex and challenging topic (Pulinets & Boyarchuk, 2004). It involves the dynamics of the earth's crust, especially in the process of the generation of electrically charged particles.

Pulinets and Boyarchuk (2004) mentioned that there is the possibility of the electric field penetrating the magnetosphere which is called as the plasmaspheric tube modification when the tube is loaned in area of earthquake preparation.

In this research, we are more focused on the concept of earthquakes; especially it's relation with the mechanism solar-dynamo process. This process involves the study on the possibility of earthquake occurrence caused by the interaction of the solar wind and geomagnetic field. On the other hand, the geomagnetic field is also caused by the induced currents in the crust, mantle and oceans. Furthermore, the magnetic field produces an electric current which circulates in the highly conductive outer core layer. This geomagnetic field is also contributing (especially, in lithosphere) towards the total geomagnetic storm produced.

CHAPTER 3: METHODOLOGY

3.1 Overview

In this chapter we outline the methodology of our research. This is a theoretical research, which requires no instrumentation. Therefore, in order to investigate the correlation between solar and seismic activities by considering the geomagnetic storm as a physical parameter requiring a large dataset to explain and examine their relationship. Hence, we collected all the data from valid international databases such as; the solar influence data analysis center (SIDC), the advanced composition explorer (ACE) spacecraft, national aeronautics space administration (NASA) via OMNIWeb data explorer and the space physics data facility and U.S geological survey (USGS). We also explained the method in order to collect the data from those databases.

3.2 Databases Centre and Data Collection

3.2.1 SIDC

The solar influences data analysis center (SIDC) is the solar physics research department at the Royal Observatory of Belgium, which includes the world data center for the sunspot number. The international sunspot number that is available from this database is among the longest running time-series of solar activity. This database provides daily, monthly and yearly sunspot number. Therefore, we used the SIDC database in order to collect the data of annual and yearly mean sunspot number in order to investigate the variation of solar activity. This database gives the annual sunspot number by taking a simple sum of the daily total sunspot number over all days of each year.

The flow chart for collecting the annual and yearly mean sunspot number by using the SIDC database are presented in Figure 3.1

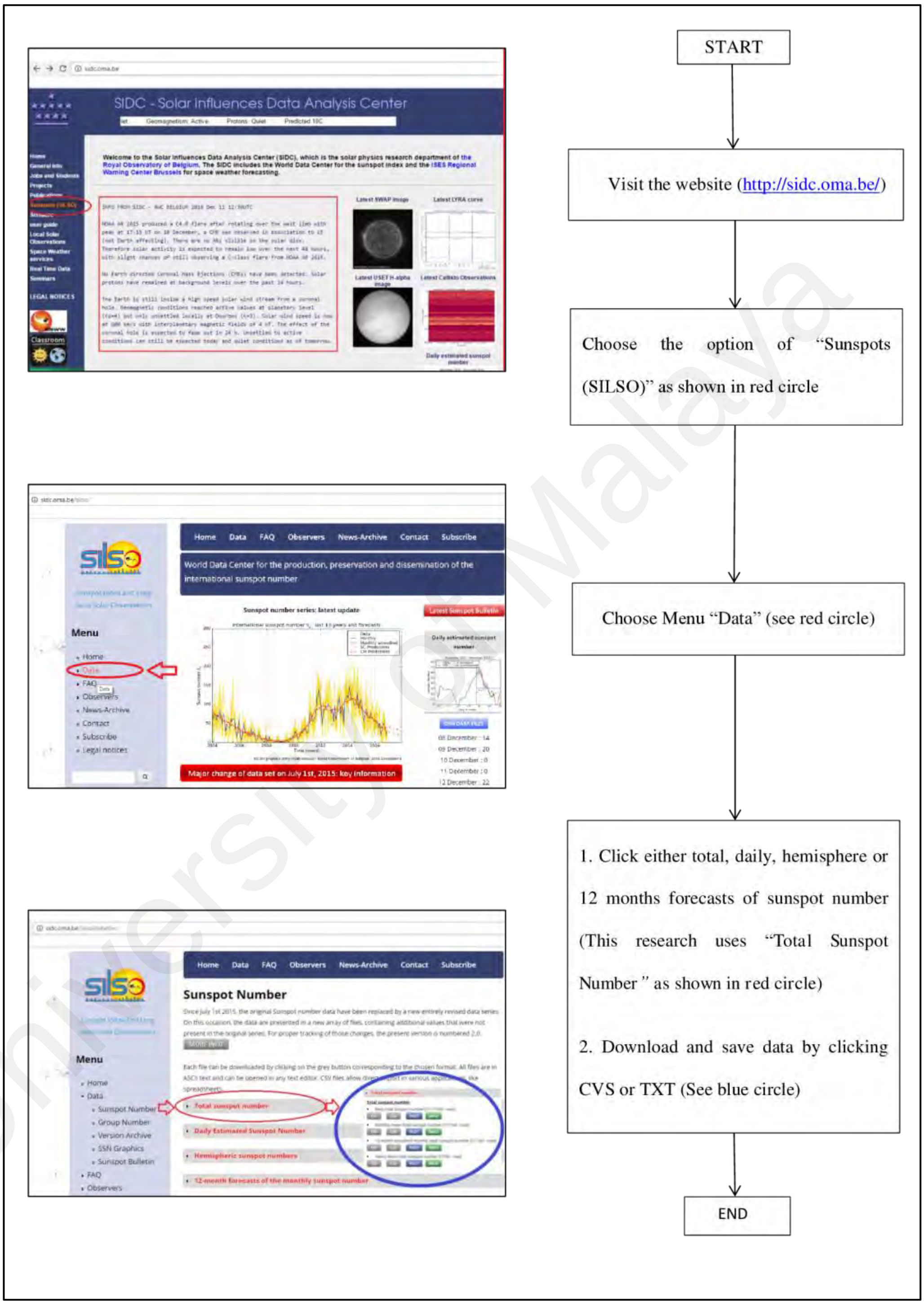

Figure 3.1: The flow chart method of collecting data of the sunspot number from SIDC database center.

3.2.2 ACE

The Advance Composition Explorer (ACE) is a mission of the National Aeronautics and Space Administration (NASA) under the Office of Space Science Mission and Payload Development Division. The ACE spacecraft has three monitoring and six high-resolution sensors that samples low and high energy particles of solar origin with a collecting power 10 to 1000 times greater than past experiments. This space mission provides several data including the solar corona, solar wind, proton density and other interplanetary particles. Hence, this research used data for solar wind parameters from the ACE database center. The flow chart of collecting the data of solar wind parameters was presented in Figure 3.2.

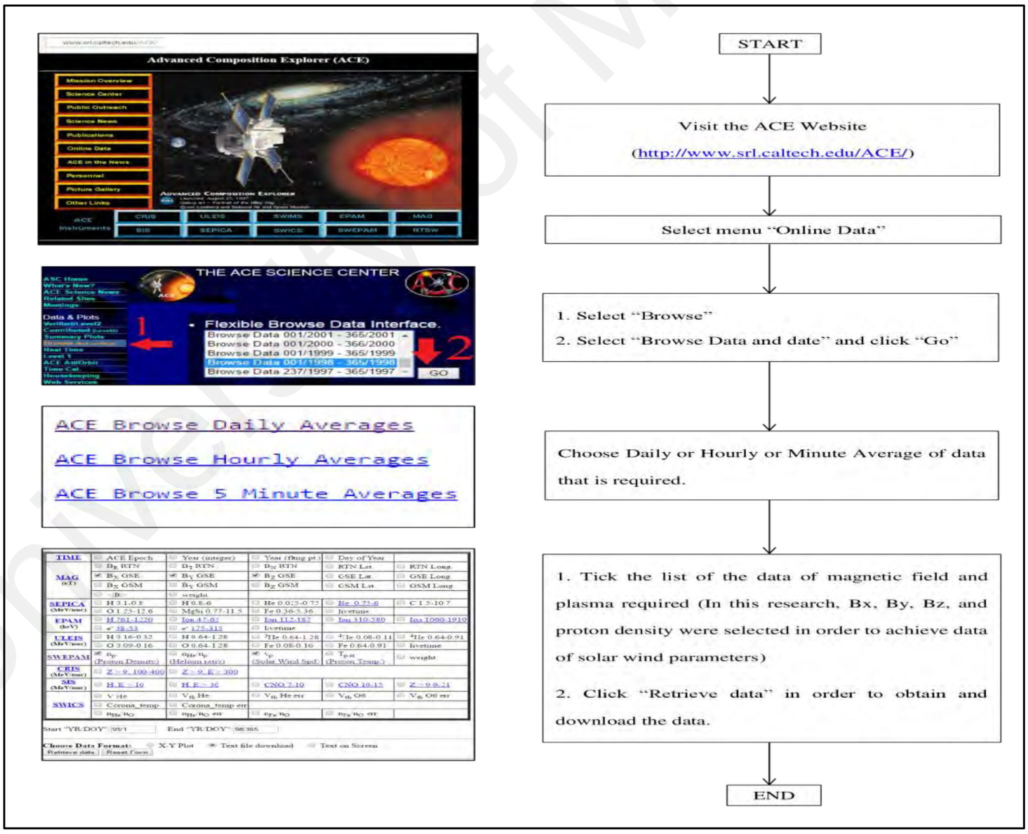

Figure 3.2: The flow chart method of collecting data for Bx, By, Bz, solar wind speed and proton density by using ACE database.

As shown in Figure 3.2, the data of solar wind parameters and Interplanetary Magnetic Field (IMF) are only available since 25^{th} of August 1997. On the other hand, one of the objectives of this research is to investigate the variation of solar wind parameters that cover from the 21^{st} up to the middle of the 24^{th} solar cycle (which is the spans the years 1976-2015). However, data for the solar wind parameters can also be obtained from the NASA's Goddard Space Flight Center via OMNIWeb Data Explorer, and the Space Physics Data Facility (Jusoh et al., 2012) (see Section 3.2.3).

3.2.3 SPDF

The Space Physics Data Facility (SPDF) is based at NASA's Goddard Space Center in Greenbelt, MD, U.S.A and also supports the science mission of NASA's Heliophysics Great Observatory. The SPDF provides data services and software in order to understand the physics and dynamics of the Heliosphere.

The SPDF also provides several data services, such as; data of current space physics via CDAWeb and data of solar wind magnetic field and plasma via OMNIWeb plus. On the other hand, SPDF via OMNIWeb also provides data of average hourly "near-earth" magnetic field and plasma magnetic field, particles of energetic proton fluxes, and solar activity and geomagnetic storm indices. Therefore, this research uses the data of the solar wind parameters (speed, dynamic pressure and input energy of the solar wind) and the geomagnetic storm indices (DST, Kp and Ap indices) from the SPDF database via OMNIWeb. The flow chart of collecting the data of solar wind parameters and geomagnetic storm indices were presented in Figure 3.3.

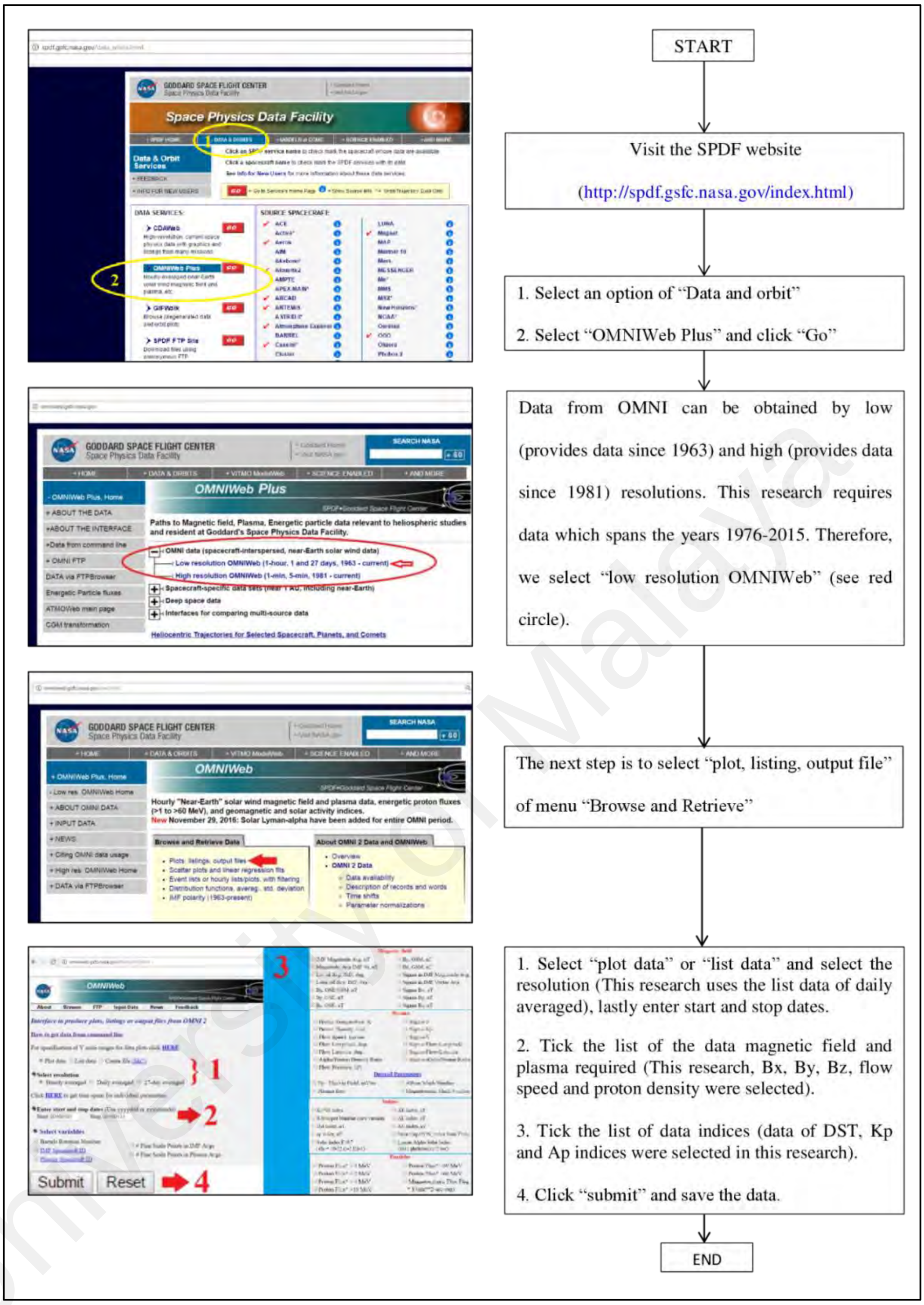

Figure 3.3: The flow chart method of collecting data solar wind parameters and geomagnetic indices by using NASA' SPDF via OMNIWeb database.

Figure 3.3 shows that the data of solar wind speed and geomagnetic storm indices (DST, Kp and Ap indices) can be obtained directly. On the other hand, data for solar wind dynamic pressure and solar wind input energy can be calculated by using Equations (2) and (3), respectively. Therefore, this research also collects data of proton density in order to obtain data of solar wind dynamic pressure. By referring those equations, this research requires to collect data of proton density and IMF magnetic field (B). All data proton density and IMF magnetic field from 1976 to 2015 were presented in Appendix.

3.2.4 USGS

The USGS (U.S Geological Survey) is a scientific agency of the United States government. This agency focuses on four major science disciplines, namely biology, geology, geography and hydrology.

This agency is in charge of several programs and one of them is the Natural Hazard Programs, which is part of the National Earthquake Hazards Reduction Program (NEHRP). This agency also provides several real-time data via the Natural Hazard Program mission, such as; volcano hazards, landslide hazard, emergency management, and earthquake hazards etc. Their scientists gather all of the data and information through periodic and continuous measurement in order to provide a view of current conditions. Therefore, this research uses the collected data for the number of earthquake occurrence from the USGS database via real-time data of earthquake hazards. The flow chart for collecting the data of earthquake was illustrated and explained in Figure 3.4.

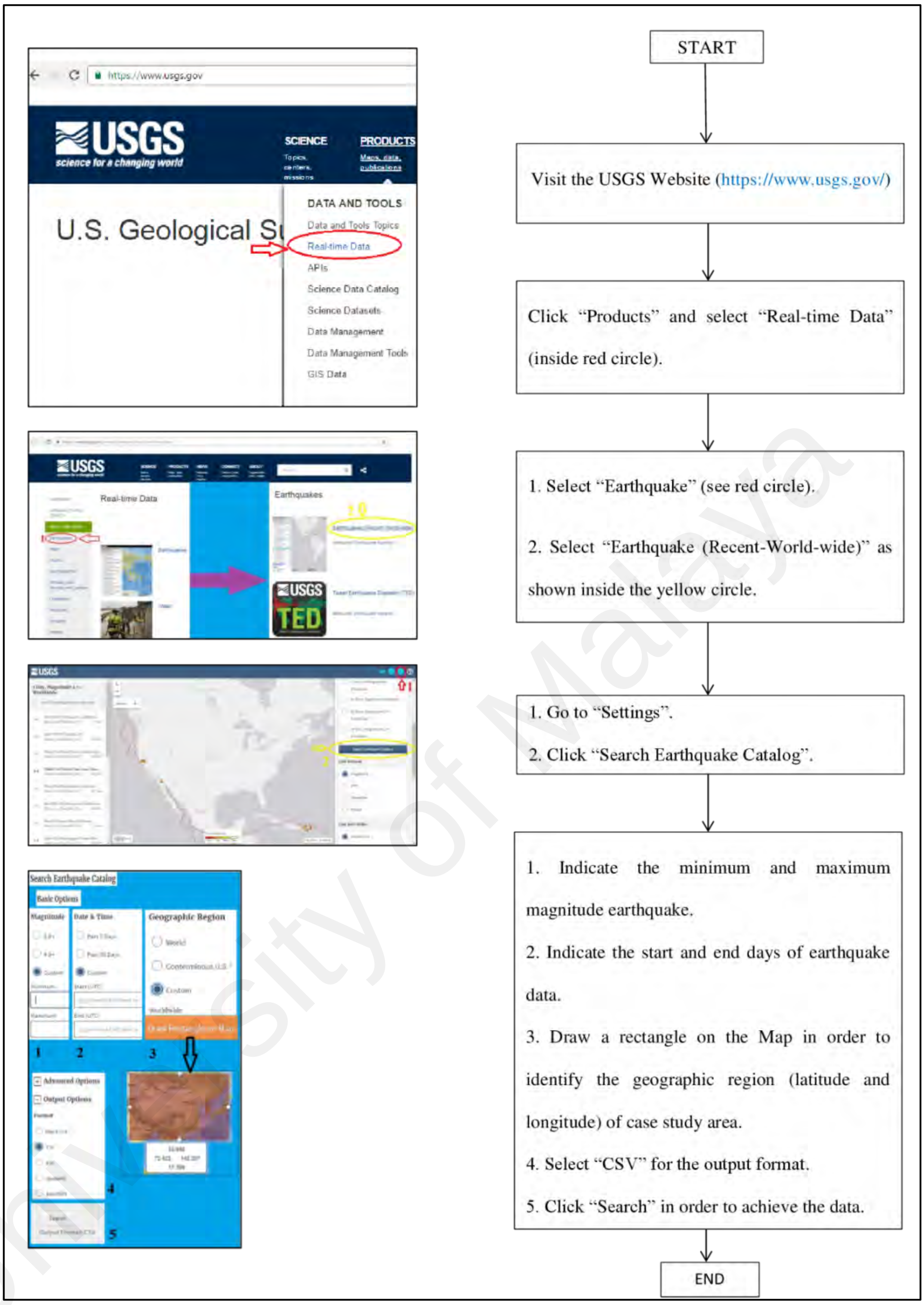

Figure 3.4: The flow chart method of collecting data of the earthquake by using USGS database center.

As mentioned in Chapter 1, the study case area of this research is localized around China and its bordering countries. From Figure 3.5, we draw and indicate the region of interest of China and its bordering countries region with latitude [17.309, 53956] and longitude [72.422, 142.207] (see Figure 3.5).

Figure 3.5 : The case study area for China and its bordering countries (bold area).

3.3 Methodology

From Figures 3.1 until 3.4, the data of annual and yearly mean sunspot number, yearly mean solar wind parameters, yearly mean geomagnetic indices, and annual number of earthquake were collected and separated by different initial year. Data of annual and yearly mean sunspot number are available since 1700, while the data of the solar wind parameters are available since 1997 and 1963 from the ACE and SPDF databases respectively. Moreover, from ONNIWeb database we collected the data of geomagnetic storm index which are available since 1976. On the other hand, based on the USGS database, data of the annual number small and large magnitude earthquakes are available since 1973 and 1901, respectively. Therefore, we collected and classified the data of sunspot number, solar wind parameters, geomagnetic indices and earthquake into different spans of the solar cycle.

This research also predicts the data of earthquakes (i.e for 2017-2019) by considering the variation of conventional and modified solar cycle. As mentioned in Chapter 2, the variation of sunspot number used in this research called as the conventional solar cycle. On the other hand, other type of solar activities such as the solar wind can also be used in order to study the variation of the solar cycle. This research used the variation of the solar wind input energy as the modified solar cycle (see Chapter 4). The model data between solar and seismic activities (see Chapter 4) does not show a linear dependence; therefore we computed and modeled their relationship by a polynomial function. For more details on polynomial function, we took references from Priestley and Chao (1972), O'Hagan and Kingman (1978), Motulsky and Ransnas (1987), Sornette et al. (2008), Dutta et al. (2013) and Srinivasamurthy et al. (2014).

Finally, by referring to Figures 3.1 until 3.5, the methodology of this research, from collecting, predicting and analysing of all the data were presented in Figure 3.6.

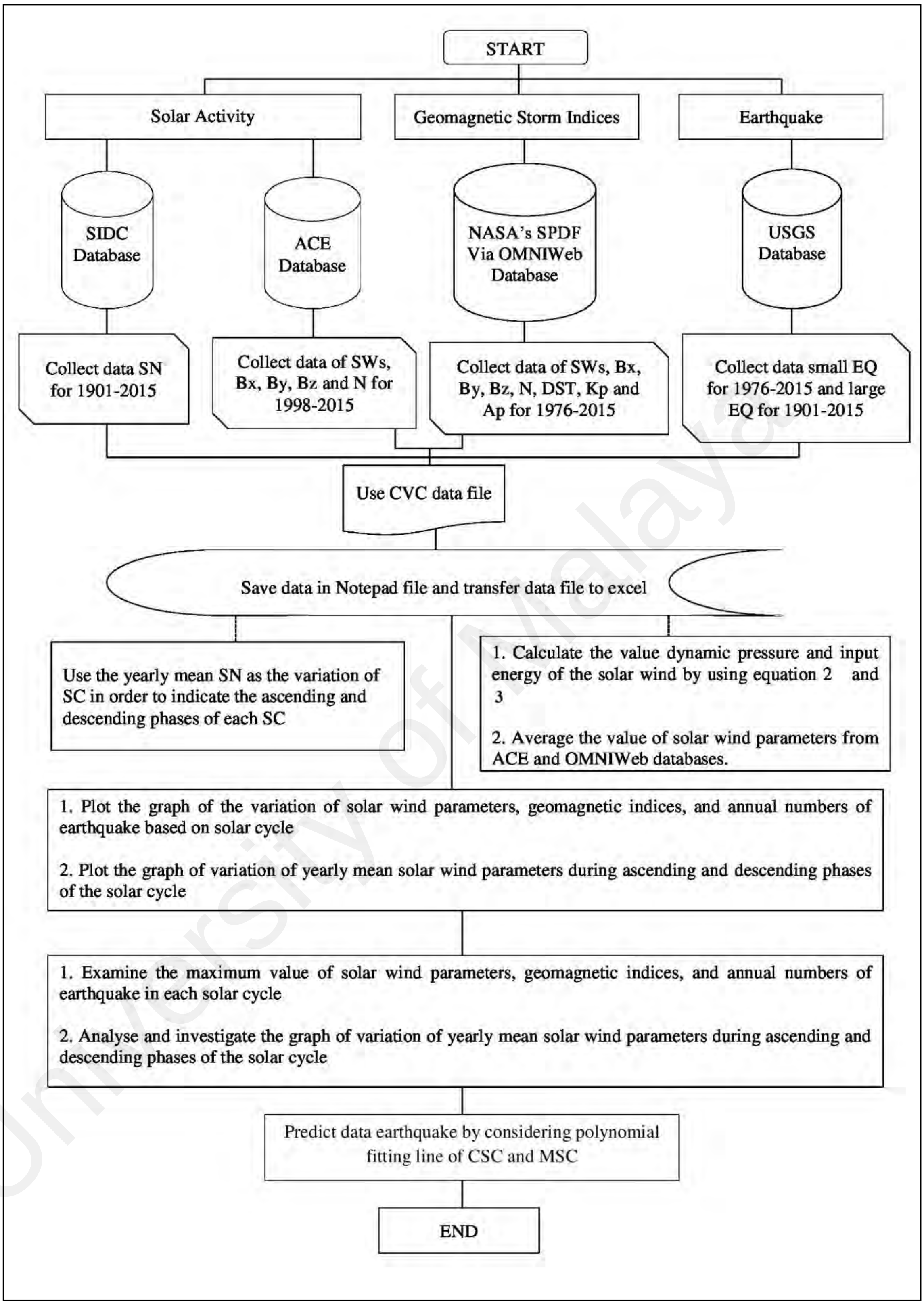

Figure 3.6: The flow chart methodology of this research.

CHAPTER 4: RESULTS AND ANALYSIS

4.1 Results

Basically, this research presents three sets of data, which are the data of solar activities, the geomagnetic storm indices and a number of earthquakes. For solar activities, we presented the data of sunspot number and data of solar wind parameters; including data of solar wind speed, solar wind dynamic pressure and solar wind input energy. We also presented the data of geomagnetic storm indices. They were used as a mediator to study the relationship between solar and seismic activities. In this research, we used the data of DST, Kp and Ap indices for studying the geomagnetic storm. Lastly, we presented the numbers of small (M<4.9) and large (M>4.9) magnitude earthquakes for China and its bordering countries region (see Figure 3.5).

4.1.1 Data of Solar Activities

4.1.1.1 Sunspot Number

In this section, we presented the data for sunspot number. Several researchers used either annual sunspot number or yearly mean value of sunspot number to investigate the variation of the solar cycle. However, our research used the yearly mean sunspot number in order to study the variation of the solar cycle. We averaged the value of annual sunspot number for each year. Hence, we presented the data of annual and yearly mean sunspot number for 115 years (1901-2015) in Table 4.1.

Table 4.1: Data for annual and yearly mean sunspot number.

Year	Annual SN	Yearly Mean SN	Year	Annual SN	Yearly Mean SN
1901	1674	4.6	1959	82165	225.1
1902	3103	8.5	1960	58201	159.0
1903	14875	40.8	1961	27897	76.4
1904	25668	70.1	1962	19473	53.4
1905	38504	105.5	1963	14580	39.9
1906	32887	90.1	1964	5501	15.0
1907	37511	102.8	1965	8020	22.0
1908	29606	80.9	1966	24366	66.8
1909	26724	73.2	1967	48511	132.9
1910	11288	30.9	1968	54905	150.0
1911	3462	9.5	1969	54519	149.4
1912	2202	6.0	1970	54016	148.0
1913	875	2.4	1971	34456	94.4
1914	5859	16.1	1972	35726	97.6
1915	28832	79.0	1973	19756	54.1
1916	34783	95.0	1974	17964	49.2
1917	63374	173.6	1975	8212	22.5
1918	49129	134.6	1976	6740	18.4
1919	38598	105.7	1977	14352	39.3
1920	22958	62.7	1978	47812	131.0
1921	15885	43.5	1979	80322	220.1
1922	8657	23.7	1980	80135	218.9
1923	3527	9.7	1981	72590	198.9
1924	10210	27.9	1982	59268	162.4
1925	27024	74.0	1983	33197	91.0
1926	38871	106.5	1984	22138	60.5
1927	41873	114.7	1985	7511	20.6
1928	47475	129.7	1986	5389	14.8
1929	39499	108.2	1987	12361	33.9
1930	21680	59.4	1988	45017	123.0
1931	12799	35.1	1989	77034	211.1
1932	6793	18.6	1990	69993	191.8
1933	3368	9.2	1991	74195	203.3
1934	5313	14.6	1992	48673	133.0
1935	21964	60.2	1993	27775	76.1
1936	48617	132.8	1994	16383	44.9
1937	69581	190.6	1995	9152	25.1
1938	66654	182.6	1996	4231	11.6
1939	54004	148.0	1997	10562	28.9
1940	41369	113.0	1998	32214	88.3

Table 4.1 continued

Year	Annual SN	Yearly Mean SN	Year	Annual SN	Yearly Mean SN
1941	28894	79.2	1999	49760	136.3
1942	18527	50.8	2000	63632	173.9
1943	9898	27.1	2001	62199	170.4
1944	5881	16.1	2002	59700	163.6
1945	20196	55.3	2003	36235	99.3
1946	56325	154.3	2004	23913	65.3
1947	78374	214.7	2005	16718	45.8
1948	70649	193.0	2006	9007	24.7
1949	69613	190.7	2007	4615	12.6
1950	43388	118.9	2008	1522	4.2
1951	35879	98.3	2009	1745	4.8
1952	16458	45.0	2010	9077	24.9
1953	7348	20.1	2011	29507	80.8
1954	2411	6.6	2012	30941	84.5
1955	19769	54.2	2013	34318	94.0
1956	73443	200.7	2014	41371	113.3
1957	98292	269.3	2015	25483	69.7
1958	95515	261.7			

4.1.1.2 Solar Wind

In this section, we presented the data of solar wind parameters, including speed, dynamic pressure and input energy of the solar wind. As mentioned in Chapter 3 (see section 3.2.3), data for the dynamic pressure and input energy of the solar wind are calculated by using equation (2) and (3). All of the data for yearly mean solar wind parameters from 1976 to 2015 were presented in Table 4.2.

Table 4.2: Data of yearly mean solar wind parameters.

Year	Yearly Mean Solar Wind Speed (SWS) (km/s)	Yearly Mean Solar Wind Dynamic Pressure (SW DynP) (nPa)	Yearly Mean Solar Wind Input Energy (ε) (Watt)
1976	386.11	2.09	2.61E+17
1977	405.89	2.28	2.32E+17
1978	423.67	2.17	5.07E+17
1979	403.08	1.86	7.52E+17
1980	391.05	1.68	5.90E+17
1981	424.82	2.04	8.12E+17
1982	364.34	2.23	9.89E+17
1983	278.39	1.63	5.27E+17
1984	275.38	1.59	5.39E+17
1985	309.92	1.82	3.39E+17
1986	323.16	1.82	3.40E+17
1987	294.62	1.74	3.64E+17
1988	295.43	1.49	6.02E+17
1989	299.68	1.63	6.68E+17
1990	278.71	1.45	6.48E+17
1991	303.28	1.94	9.90E+17
1992	283.14	1.88	7.24E+17
1993	308.95	1.84	4.43E+17
1994	354.36	1.77	4.10E+17
1995	427.09	2.37	4.07E+17
1996	421.02	2.18	2.41E+17
1997	405.89	2.28	2.35E+17
1998	410.27	1.97	6.52E+17
1999	438.82	1.77	6.15E+17
2000	447.83	1.88	7.24E+17
2001	425.88	1.77	7.65E+17
2002	439.80	1.95	8.35E+17
2003	540.23	2.31	9.89E+17
2004	451.42	1.81	7.21E+17
2005	472.96	2.07	6.10E+17
2006	430.97	1.81	2.92E+17
2007	441.12	1.63	1.92E+17
2008	450.60	1.48	1.89E+17
2009	364.60	1.25	1.29E+17
2010	403.60	1.38	2.51E+17
2011	420.79	1.47	3.19E+17
2012	408.36	1.48	5.27E+17
2013	396.99	1.41	3.92E+17
2014	398.28	1.56	3.70E+17
2015	437.36	2.16	5.79E+17

4.1.2 Data of Geomagnetic Storm Index

In this section, we presented the data of the mediator for studying the correlation between solar and seismic activities. We presented three classifications of geomagnetic storm indices, which are; DST, Kp and Ap indices. As well as solar wind parameters, we also presented the yearly mean data of geomagnetic storm indices (DST, Kp and Ap indices) in Table 4.3.

Table 4.3: Data for annual and yearly mean of disturbance storm time (DST), 3-hour interplanetary (Kp) and average planetary (Ap) indices.

Year	Yearly Mean DST index	Yearly Mean Kp Index	Yearly Mean Ap Index
1976	-13.5	22.4	12.9
1977	-17.0	21.4	11.9
1978	-22.1	25.0	16.9
1979	-16.0	24.5	14.5
1980	-11.5	20.9	11.1
1981	-24.4	25.8	16.3
1982	-23.5	30.6	22.4
1983	-17.1	28.2	18.5
1984	-17.4	28.5	18.8
1985	-15.8	23.5	13.7
1986	-15.6	21.6	12.5
1987	-11.8	20.7	10.9
1988	-19.9	22.5	12.7
1989	-29.8	27.7	19.5
1990	-21.0	25.5	16.2
1991	-30.7	30.2	23.4
1992	-20.2	25.8	16.5
1993	-17.7	24.4	15.0
1994	-21.3	27.4	18.1
1995	-16.8	21.6	12.6
1996	-10.9	18.9	9.3
1997	-14.5	16.3	8.4
1998	-17.0	20.2	12.0
1999	-13.1	21.9	12.5
2000	-19.0	23.6	15.0
2001	-17.7	21.0	12.9
2002	-21.0	22.6	13.1
2003	-22.1	30.7	21.8

Table 4.3 continued

Year	Yearly Mean DST index	Yearly Mean Kp Index	Yearly Mean Ap Index
2004	-12.2	21.8	13.4
2005	-16.3	21.5	13.5
2006	-11.7	16.1	8.5
2007	-8.2	15.1	7.5
2008	-7.8	14.6	6.9
2009	-2.9	9.0	3.9
2010	-9.5	12.6	6.0
2011	-11.2	14.9	7.5
2012	-8.3	16.8	9.1
2013	-7.8	14.8	7.6
2014	-6.7	16.3	7.7
2015	-15.1	21.2	12.2

4.1.3 Data of Earthquakes

In this section, we presented the data for the annual number of small magnitude (M<4.9) and large magnitude (M>4.9) earthquakes (see Table 4.4). As we have mentioned in Chapter 3, data for the small magnitude earthquakes were only available since 1976. Hence, as presented in Table 4.4, data for an annual number of small magnitude earthquakes were presented from the year of 1976 until 2015, while the data of the annual number of large magnitude earthquakes were presented from 1901 until 2015.

Table 4.4: Annual numbers of small and large magnitude earthquakes.

Year	M<4.9	M>4.9	Year	M<4.9	M>4.9
1901	-	1	1959	-	40
1902	-	1	1960	-	21
1903	-	0	1961	-	41
1904	-	0	1962	-	30
1905	-	3	1963	-	44
1906	-	3	1964	-	31
1907	-	0	1965	-	31
1908	-	3	1966	-	45
1909	-	0	1967	-	31

Table 4.4 continued

Year	M<4.9	M>4.9	Year	M<4.9	M>4.9
1910	-	2	1968	-	27
1911	-	4	1969	-	29
1912	-	1	1970	-	27
1913	-	1	1971	-	56
1914	-	2	1972	-	53
1915	-	3	1973	-	139
1916	-	1	1974	-	152
1917	-	2	1975	-	181
1918	-	3	1976	357	176
1919	-	2	1977	287	130
1920	-	5	1978	415	170
1921	-	1	1979	388	98
1922	-	9	1980	436	133
1923	-	15	1981	372	109
1924	-	9	1982	479	144
1925	-	5	1983	541	202
1926	-	5	1984	474	167
1927	-	7	1985	775	224
1928	-	3	1986	716	204
1929	-	5	1987	532	177
1930	-	11	1988	577	141
1931	-	11	1989	646	158
1932	-	3	1990	676	169
1933	-	5	1991	666	96
1934	-	8	1992	777	140
1935	-	11	1993	721	145
1936	-	5	1994	494	121
1937	-	13	1995	1029	122
1938	-	15	1996	1286	124
1939	-	6	1997	982	130
1940	-	4	1998	1038	105
1941	-	5	1999	964	122
1942	-	6	2000	1579	204
1943	-	5	2001	1008	130
1944	-	8	2002	1153	108
1945	-	6	2003	1224	148
1946	-	6	2004	1487	149
1947	-	4	2005	1560	174
1948	-	9	2006	1611	112
1949		4	2007	1616	154
1950	-	74	2008	3510	250

Table 4.4 continued

Year	M<4.9	M>4.9	Year	M<4.9	M>4.9
1951	-	68	2009	659	137
1952	-	39	2010	779	133
1953	-	37	2011	2296	464
1954	-	35	2012	1171	164
1955	-	41	2013	1152	171
1956	-	29	2014	1397	137
1957	-	24	2015	1449	142
1958	-	48			

4.2 Analysis

4.2.1 Variation of sunspot number

In order to examine and investigate the solar cycle variation, this research plotted the data of yearly mean sunspot number presented in Table 4.1. The variations of the yearly mean sunspot numbers from 1901 up to the end of 2015 are illustrated in Figure 4.1.

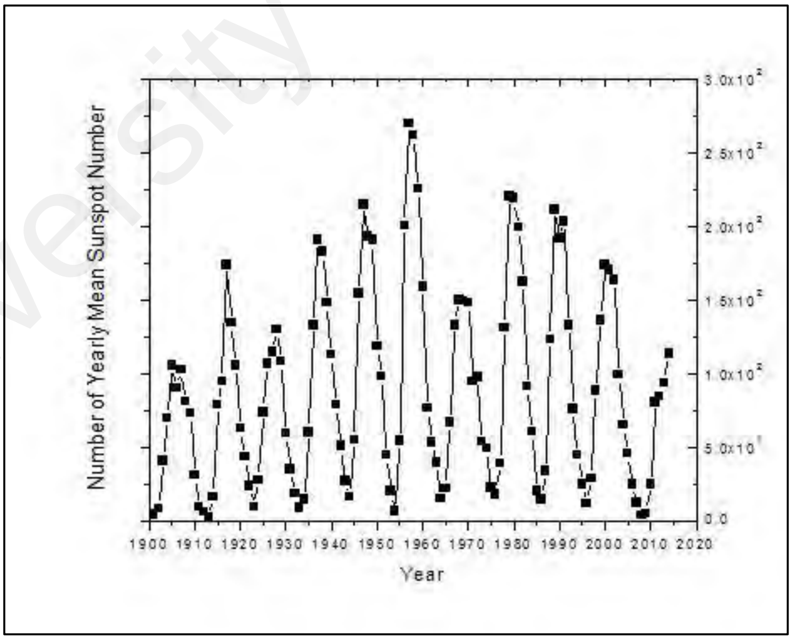

Figure 4.1: The variation of sunspot number (SN) for 114 years (1901-2015).

From Figure 4.1, we found that the whole 114 years (1901-2015) covers about ±11 solar cycles (14^{th} up to the middle of the 24^{th} solar cycle), while Khodairy et al. (2015) mentioned that the 1^{st} solar cycle begins in 1775. From figure 4.1, we also found that one solar cycle takes about ±11 years of variation in sunspot number. However, for every solar cycle, we found that the variation of sunspot number for the ascending phase varies about ±5 years, while for the descending phase takes about ±7 years (Khain & Khalilov, 2007).

4.2.2 The Variation of Solar Wind Parameters, Geomagnetic Storm Indices and Annual Numbers of Earthquake Based On Solar Cycle

4.2.2.1 The variation of solar wind parameters

As mentioned in Chapter 1 that the solar wind transfers energy into the earth magnetic field. However, the interaction between the solar wind and earth's magnetic field will affect the ionospheric current and tectonic plate movement. Hence, in order to investigate the correlation between solar and seismic activities, we plotted and analysed the trend of solar wind speed, solar wind dynamic pressure and solar wind input energy based on the variation of the solar cycle. By referring to Figure 4.1, the data of solar wind parameters that were presented in Table 4.2 covers about ±4 solar cycles (21^{st} up to the middle of the 24^{th} solar cycle). Hence, we presented the variations of solar wind parameters during the 21^{st} up to the middle of the 24^{th} solar cycle in Figures 4.2 until 4.5.

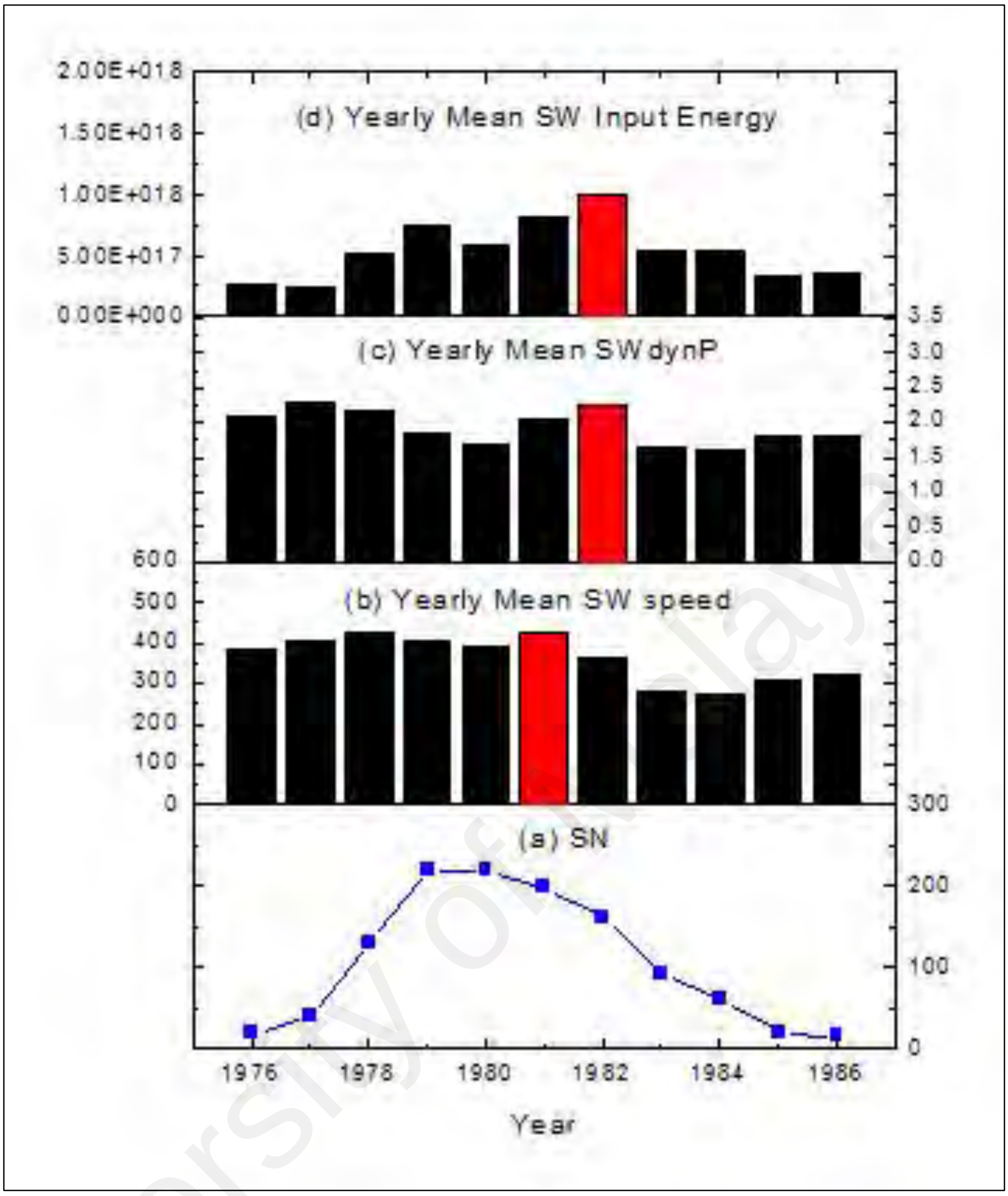

Figure 4.2: The variation of yearly mean sunspot number (a), yearly mean solar wind speed (SWS) (km/s) (b), yearly mean solar wind dynamic pressure (SW DynP) (nPa) and (c) yearly mean solar wind input energy (SW ε) (Watt or Erg/s) during 21st solar cycle.

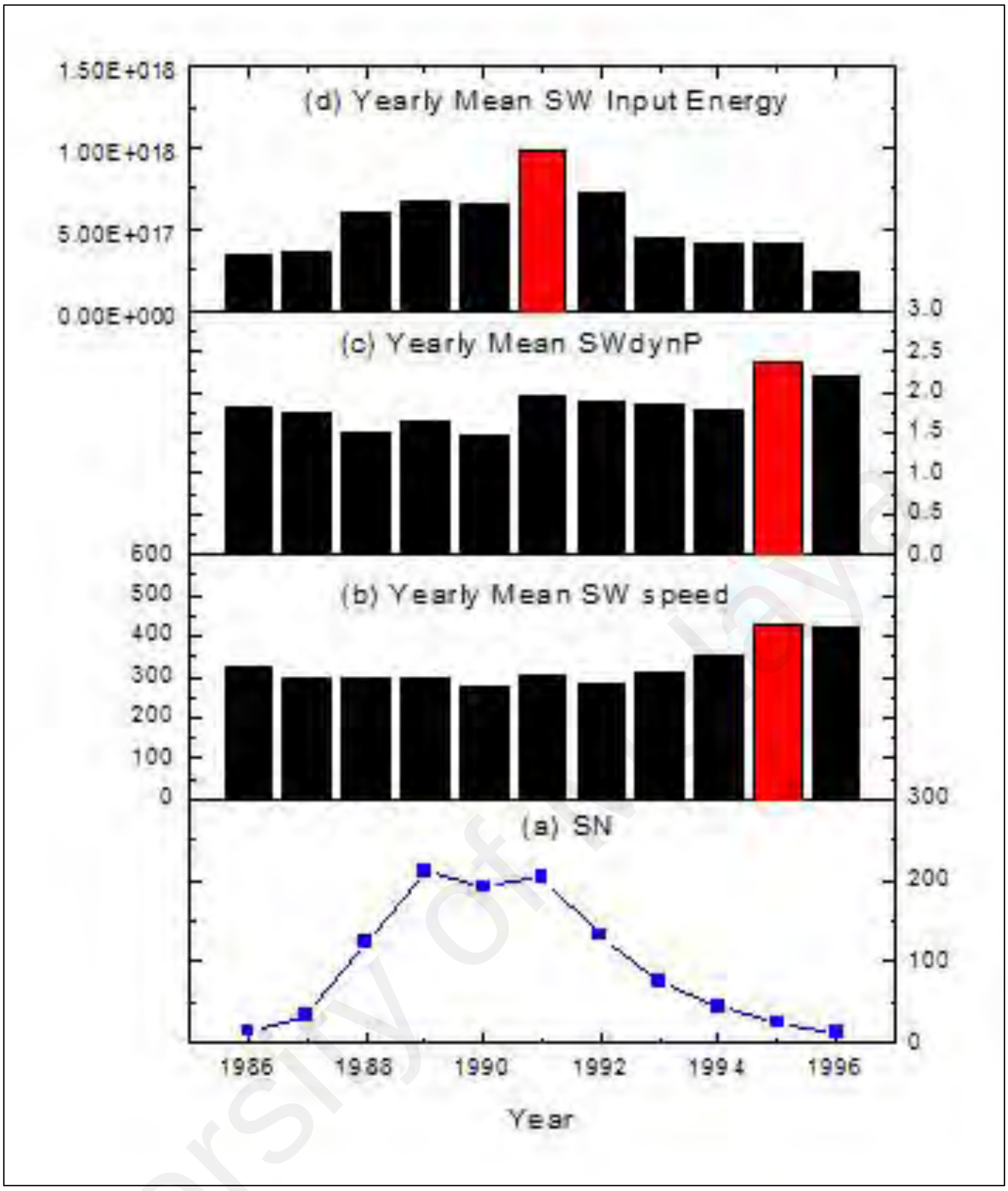

Figure 4.3: The variation of yearly mean sunspot number (a), yearly mean solar wind speed (SWS) (km/s) (b), yearly mean solar wind dynamic pressure (SW DynP) (nPa) and (c) yearly mean solar wind input energy (SW ε) (Watt or Erg/s) during 22nd solar cycle.

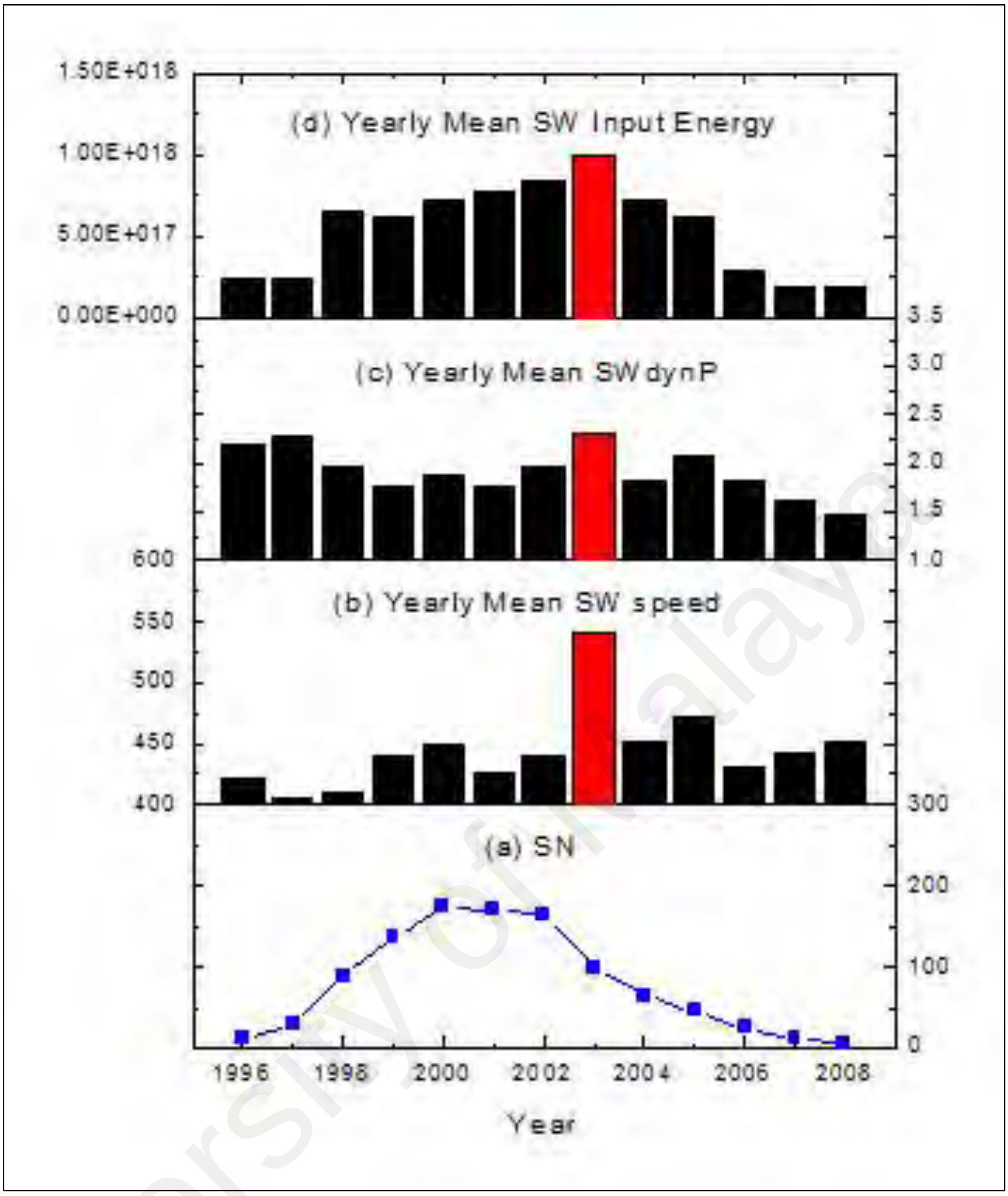

Figure 4.4: The variation of yearly mean sunspot number (a), yearly mean solar wind speed (SWS) (km/s) (b), yearly mean solar wind dynamic pressure (SW DynP) (nPa) and (c) yearly mean solar wind input energy (SW ε) (Watt or Erg/s) during 23rd solar cycle.

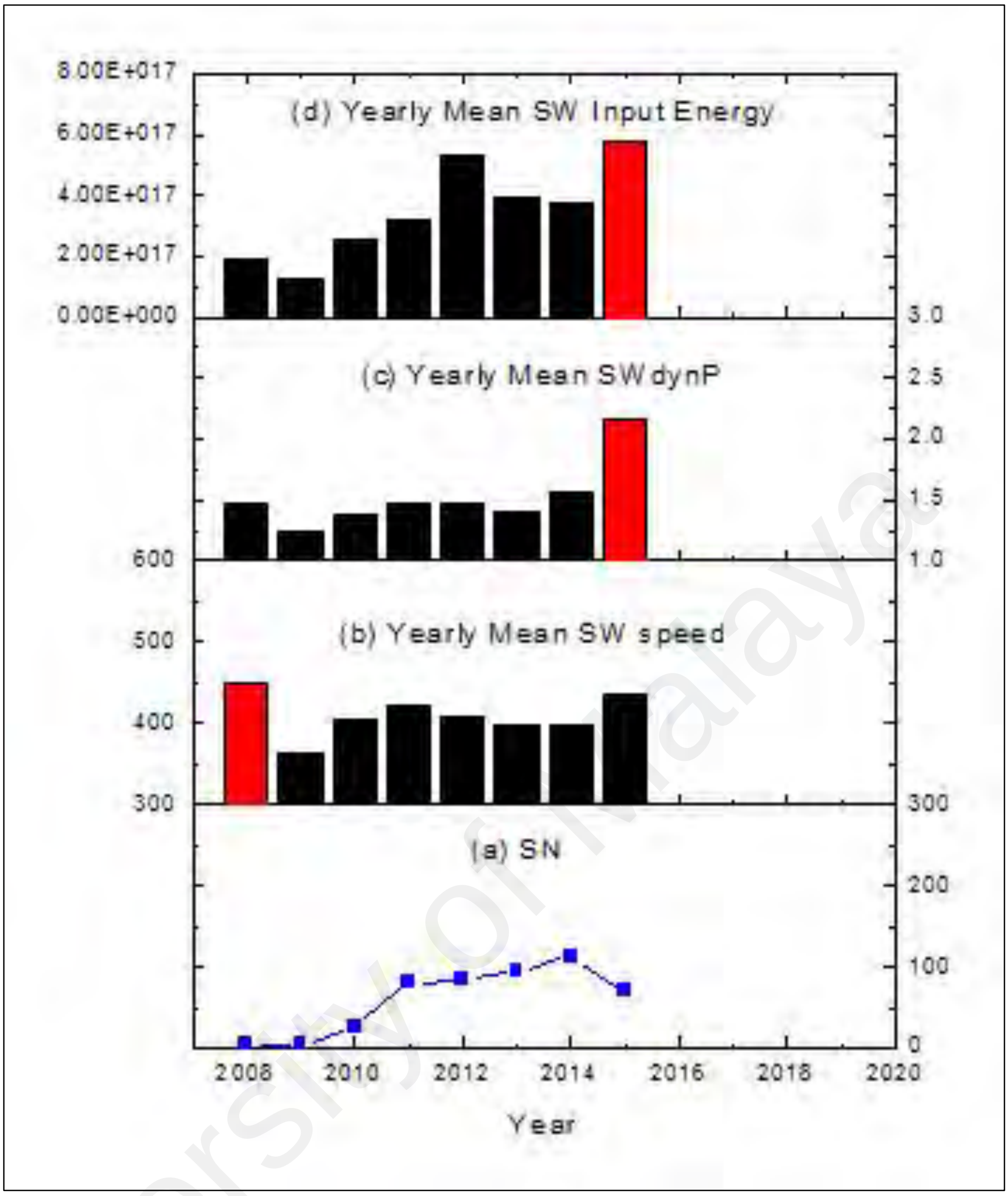

Figure 4.5: The variation of yearly mean sunspot number (a), yearly mean solar wind speed (SWS) (km/s) (b), yearly mean solar wind dynamic pressure (SW DynP) (nPa) and (c) yearly mean solar wind input energy (SW ε) (Watt or Erg/s) during middle of 24^{th} solar cycle.

The red bar charts in Figures 4.2 until 4.5 indicated as the maximum value for solar wind speed, solar wind dynamic pressure and solar wind input energy in each solar cycle. Those figures show that the maximum values of the solar wind speed during the 21^{st} up to the middle of the 24^{th} solar cycles were found in 1981, 1995, 2003 and 2008, respectively. For the same solar cycles, the maximum values of solar wind dynamic pressure were found in 1982, 1995, 2003 and 2015. On the other hand, the maximum values of solar wind input energy were found in the year 1982, 1991, 2003 and 2015.

Hence, we suggested that the maximum peak value for solar wind speed, solar wind dynamic pressure and solar wind input energy were found during the years of descending phase of the solar cycle.

4.2.2.2 The variation of geomagnetic storm indices

In order to use the inclusion of geomagnetic storm in understanding the correlation between solar and seismic activities, we plotted and analysed the trend of DST, Kp and Ap indices based on the variation of the solar cycle. By considering Figure 4.1, the data of geomagnetic storm indices that were presented in Table 4.3 covers about ±4 solar cycles (21^{st} up to the middle of the 24^{th} solar cycle). Hence, we presented the variations of geomagnetic storm indices during the 21^{st} up to the middle of the 24^{th} solar cycle (see Figures 4.6 until 4.9).

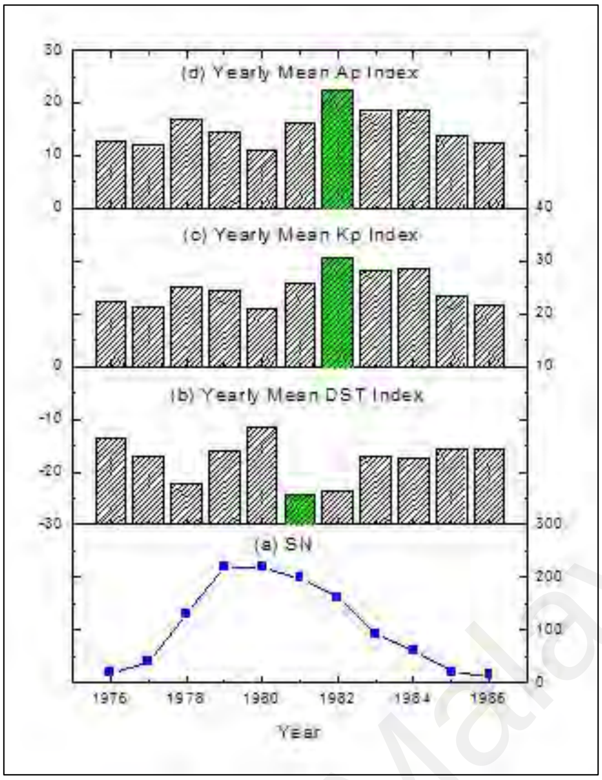

Figure 4.6: The variation of yearly mean sunspot number (a), yearly mean DST index (b), yearly mean Kp index and (c) yearly mean Ap index during 21st solar cycle.

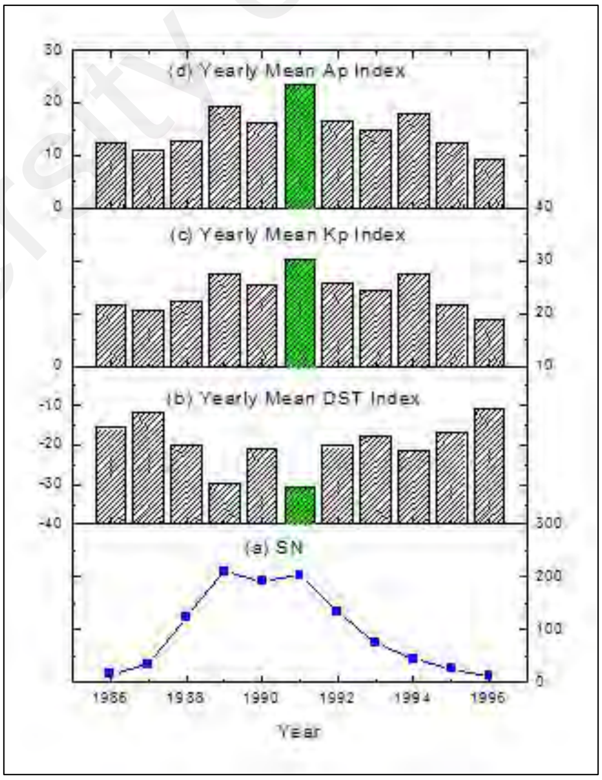

Figure 4.7: The variation of yearly mean sunspot number (a), yearly mean DST index (b), yearly mean Kp index and (c) yearly mean Ap index during 22nd solar cycle.

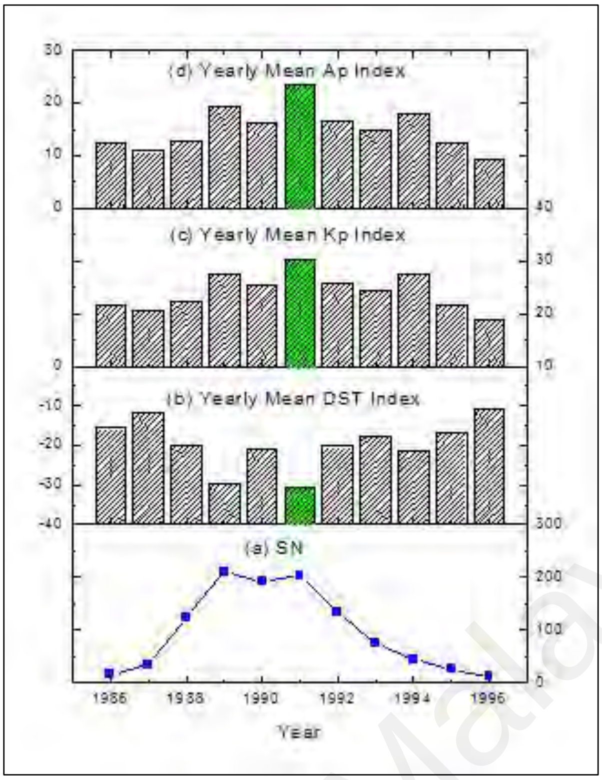

Figure 4.8: The variation of yearly mean sunspot number (a), yearly mean DST index (b), yearly mean Kp index and (c) yearly mean Ap index during 23rd solar cycle.

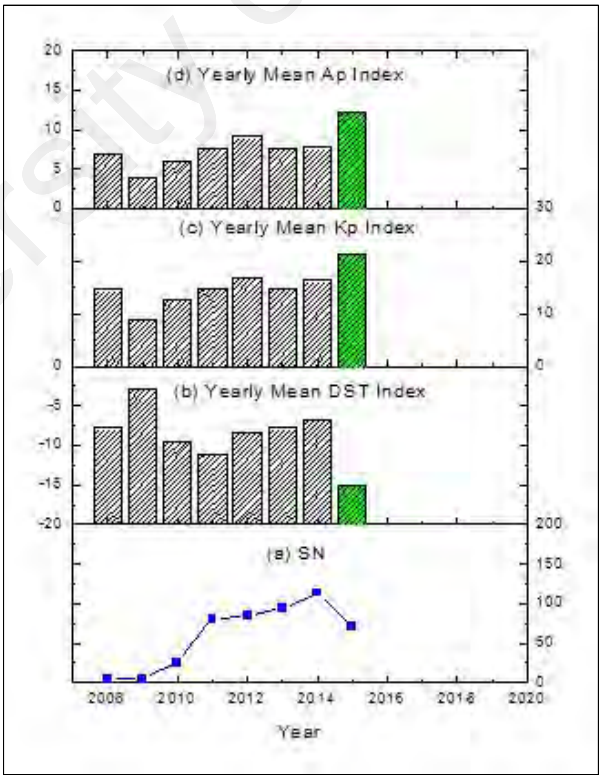

Figure 4.9: The variation of yearly mean sunspot number (a), yearly mean DST index (b), yearly mean Kp index and (c) yearly mean Ap index during middle of 24th solar cycle.

The green bar charts in Figures 4.6 until 4.9 indicate as the maximum value for DST, Kp and Ap indices in each solar cycle. Those figures show that during the 21st up to the middle of 24th of the solar cycle, the maximum peak value of the DST index were found in 1981, 1991, 2003 and 2015, respectively. On the other hand, the maximum peak value of Kp index during the 21st up to the middle of the 24th solar cycle were found in the year 1982, 1991, 2003 and 2015, respectively. At the same solar cycle, the maximum peak value of Ap index was found in the year 1982, 1991, 2003 and 2015, respectively. Hence, we suggest that for each solar cycle, the maximum peak value for DST, Kp and Ap indices were found in years of the descending phase of the solar cycle.

4.2.2.3 The variation of annual number of earthquake

From section 4.2.2.1 and 4.2.2.2, we mentioned that for each solar cycle, the maximum value of solar wind parameters and geomagnetic indices were found during the descending phase of the solar cycle (from the 21st up to the middle of the 24th solar cycle). In this section, we also analysed the variation in annual numbers of small ($M<4.9$) and large ($M>4.9$) magnitude earthquakes based on variation solar cycle. We also investigated the maximum peak value of small and large magnitudes earthquakes in every solar cycle.

By considering Figure 4.1, the annual numbers of large magnitude earthquakes that were presented in Table 4.4 cover about ±11 solar cycles (14th up to the middle of the 24th solar cycle). However, the annual numbers of small magnitude earthquake cover only about ±4 solar cycles (21st up to the middle of the 24th solar cycle). Hence, we plotted the variation of annual small (see Figures 4.10 until 4.13) and large (see Figures 4.14 until 4.24) magnitude earthquakes during those solar cycles.

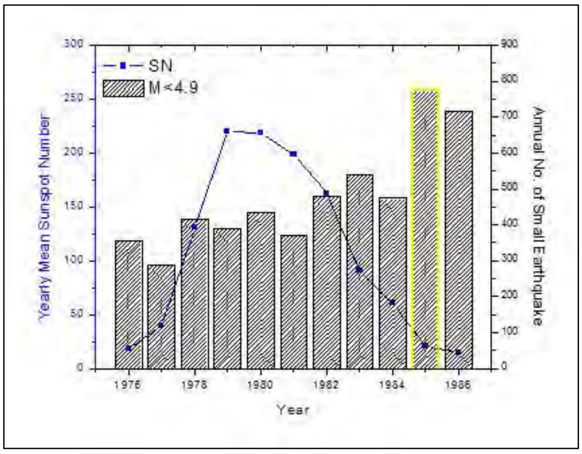

Figure 4.10: The variation of an annual number of small magnitude earthquakes during the 21st solar cycle.

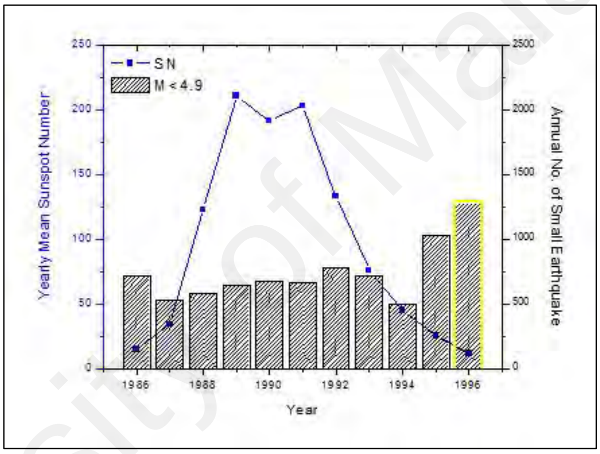

Figure 4.11: The variation of an annual number of small magnitude earthquakes during the 22nd solar cycle.

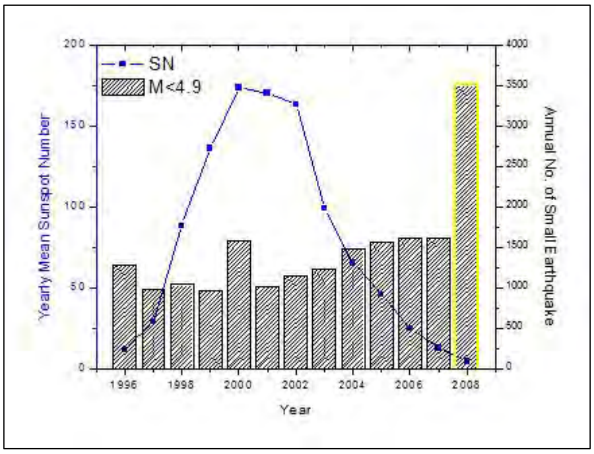

Figure 4.12: The variation of an annual number of small magnitude earthquakes during the 23rd solar cycle.

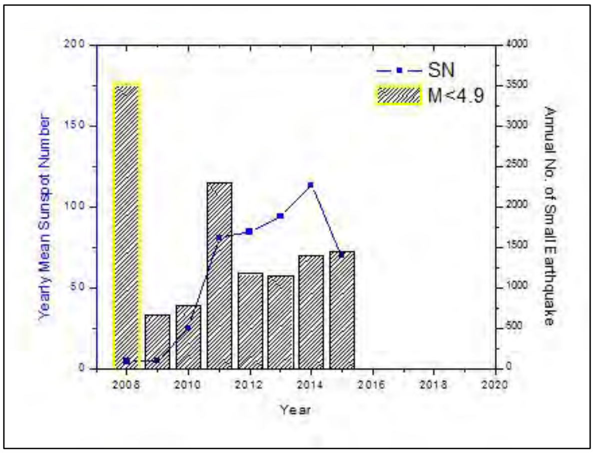

Figure 4.13: The variation of an annual number of small magnitude earthquakes during the middle of the 24th solar cycle.

The yellow lines in bar charts presented in Figure 4.10 to 4.13 indicate as the maximum value for the annual number of small magnitude earthquakes in each solar cycle. Those Figures show the annual variations of small magnitude earthquakes are at the same solar cycle as the solar wind parameters and geomagnetic indices, which are during the 21st until the middle of the 24th solar cycle. From Figures 4.10 and 4.11, the maximum value of annual small magnitude earthquakes during the 21st and 22nd solar cycles was found in the year 1985 and 1986, respectively. On the other hand, for both of the 23rd and half of 24th solar cycle, the maximum peak value of small magnitude earthquakes was found in the same year, that is 2008 (see Figures 4.12 and 4.13). Hence, we also suggest that the maximum value of an annual number of small magnitude earthquake during 21st up to the middle of the 24th solar cycle were found during descending phase except during 24th solar cycle. The 24th solar cycle is still ongoing, while Ajabshirizadeh et al., (2011) were predicted that the last minimum year for the 24th solar cycle is predicted on year around 2018 or 2019.

As mentioned before, data for the annual numbers of large magnitude earthquakes were available since 1901 until 2015 (see Table 4.4). Hence, we analysed, investigated and plotted their variation during the 14th up to the middle of the 24th solar cycle (see Figures 4.14 until 4.24).

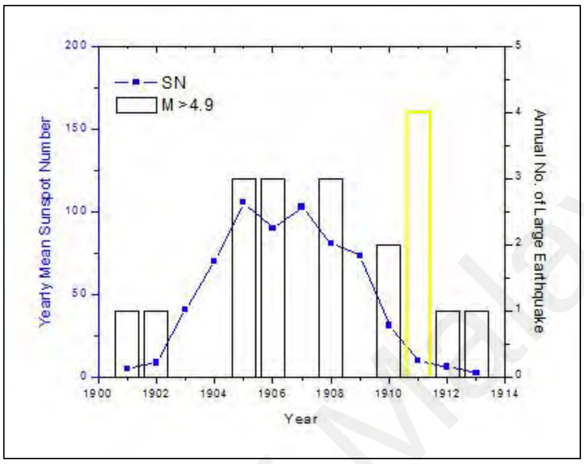

Figure 4.14: The variation of annual of large magnitude earthquake during 14th solar cycle.

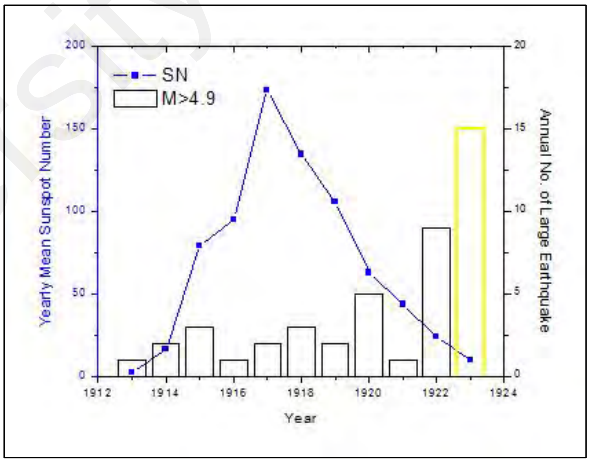

Figure 4.15: The variation of annual of large magnitude earthquake during 15th solar cycle.

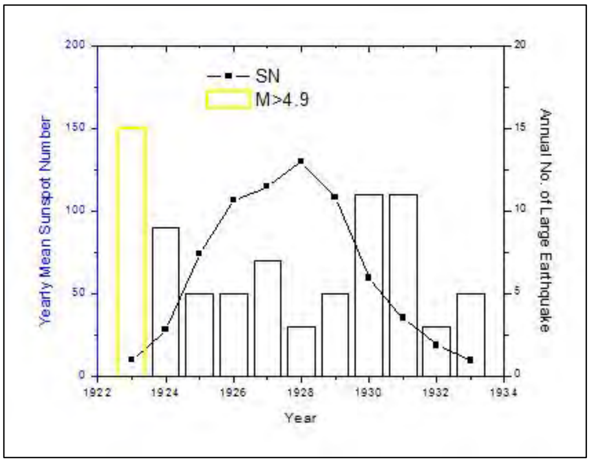

Figure 4.16: The variation of annual of large magnitude earthquake during 16th solar cycle.

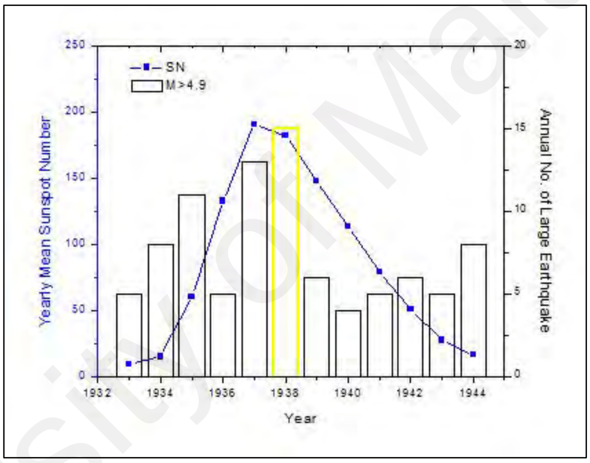

Figure 4.17: The variation of annual of large magnitude earthquake during 17th solar cycle.

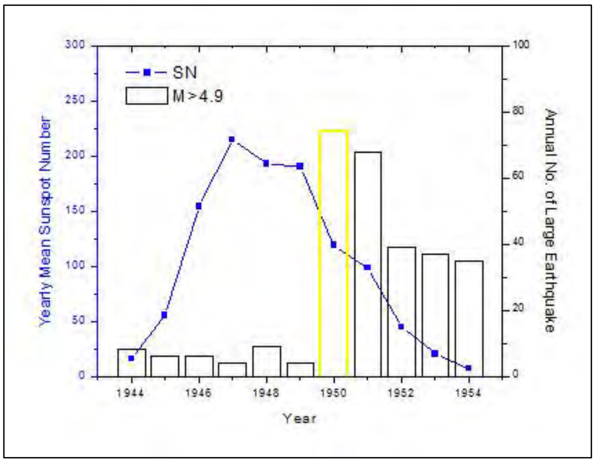

Figure 4.18: The variation of annual of large magnitude earthquake during 18th solar cycle.

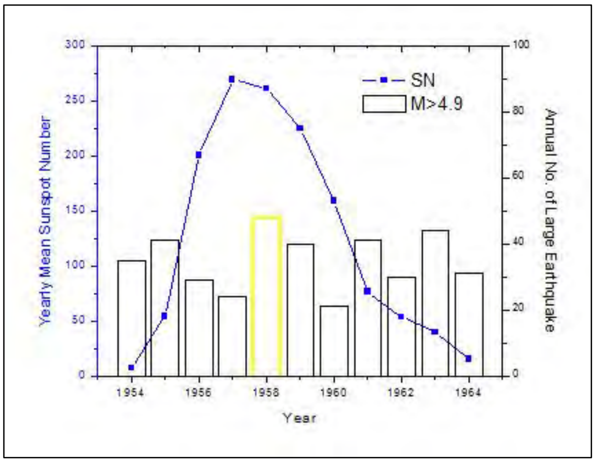

Figure 4.19: The variation of annual of large magnitude earthquake during 19th solar cycle.

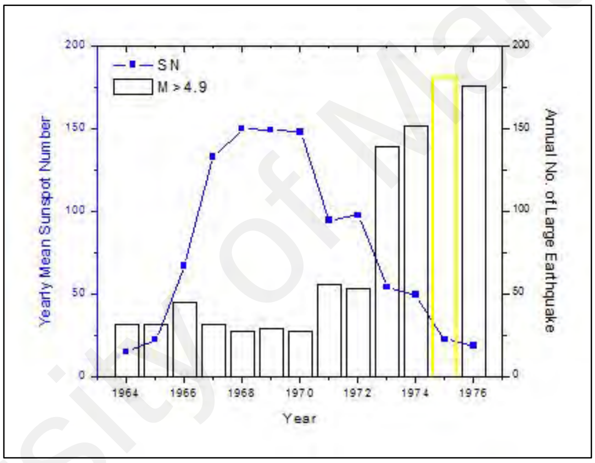

Figure 4.20: The variation of annual of large magnitude earthquake during 20th solar cycle.

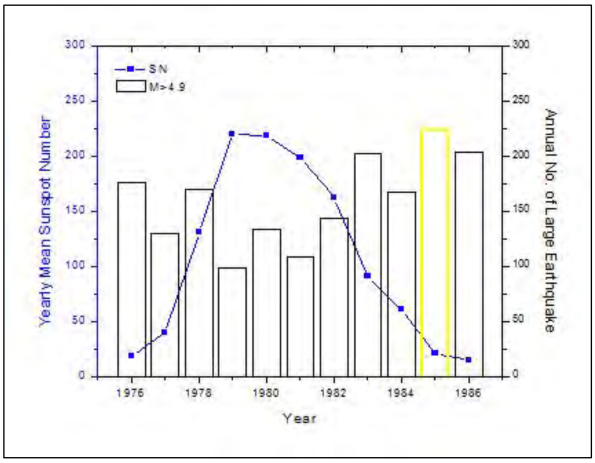

Figure 4.21: The variation of annual of large magnitude earthquake during 21st solar cycle.

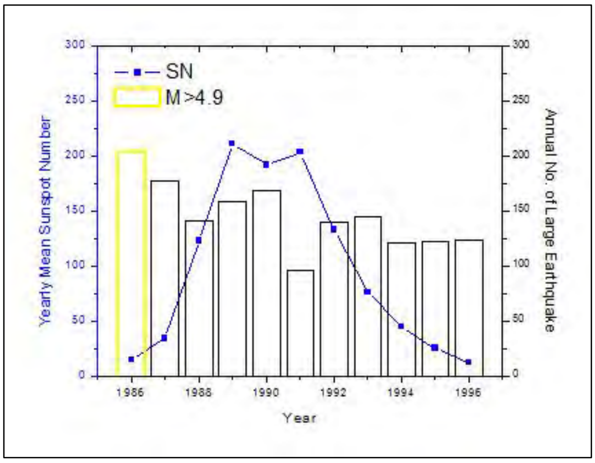

Figure 4.22: The variation of annual of large magnitude earthquake during 22nd solar cycle.

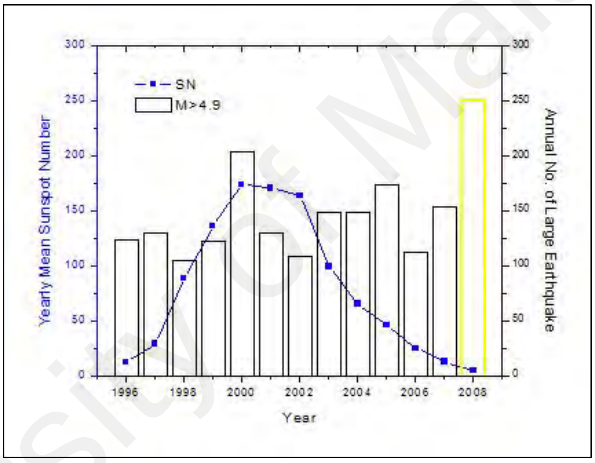

Figure 4.23: The variation of annual of large magnitude earthquake during 23rd solar cycle.

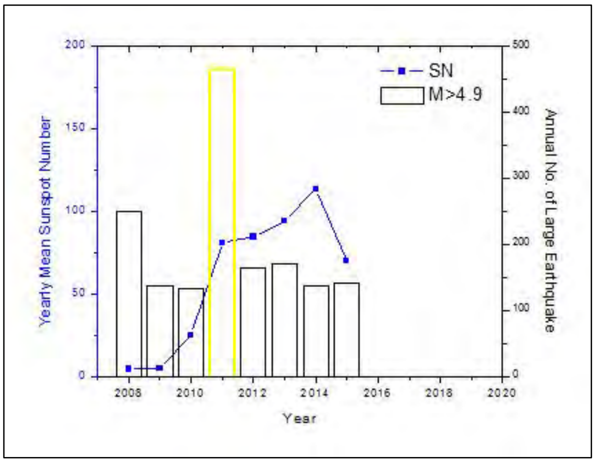

Figure 4.24: The variation of annual of large magnitude earthquake during middle of 24th solar cycle.

The yellow lines in bar charts illustrated in Figures 4.14 until 4.24 indicate the maximum value for the annual number of large magnitude earthquakes in each solar cycle from the 14^{th} up to the middle of 24^{th}. Table 4.5 shows the peak values of large magnitude earthquakes by year, it was found that the maximum annual number of large magnitude earthquakes during those solar cycles were found in 1911, 1923, 1938, 1950, 1958, 1975, 1985, 1986, 2008 and 2011. Note that the 15^{th} and 16^{th} solar cycles overlap in 1923. All the years presented were during the descending phase except for 1923 (see Figure 4.16) and 1986 (see Figure 4.22). Hence, we suggest that from the 14^{th} up to the middle of the 24^{th} solar cycle (excluding the 16^{th} and 22^{nd} solar cycles), the maximum annual number of large magnitude earthquakes were found during the years of the descending phase.

Table 4.5: The year of maximum value number of large magnitude earthquake.

Solar Cycle	Year of max peak value
14^{th}	1911
15^{th}	1923
16^{th}	1923
17^{th}	1938
18^{th}	1950
19^{th}	1958
20^{th}	1975
21^{st}	1985
22^{nd}	1986
23^{rd}	2008
24^{th}	2011

From our analysis and investigation, we suggest that the maximum value of the solar wind parameters (speed, dynamic pressure and input energy of solar wind), geomagnetic storm indices (DST, Kp, and Ap indices) and annual number of earthquakes (both of small and large magnitudes) for every solar cycle were found during the year of descending phase.

4.2.3 The Variation of the Solar Wind Parameters, Geomagnetic Storm Index and Earthquake during Ascending and Descending Phases of Each Solar Cycle

From section 4.2.2, we mentioned that the maximum peak value for solar wind parameters, geomagnetic indices and an annual number of small and large magnitude earthquakes were found during the descending phases of the solar cycle. Therefore we are motivated to analyse and investigate their variation by considering the ascending and descending phases of each solar cycle. Hence, by referring to Tables 4.1until 4.4, all of the data of solar activities, geomagnetic storm indices and a number of earthquakes during ascending and descending phases of the solar cycle are presented in Tables 4.6 and 4.7, respectively.

For further investigation, by referring to Tables 4.6 and 4.7, we plotted the graphs in order to examine the variations of solar wind parameters, geomagnetic storm indices and an annual number of earthquakes during the ascending and descending phases of the solar cycle.

Firstly, we plotted and analysed the graphs of yearly mean solar wind parameters by considering the ascending and descending phases of the 21^{st} up to the middle of the 24^{th} solar cycles. This research has found that the variation of the yearly mean solar wind speed (see Figure 4.25), solar wind dynamic pressure (see Figure 4.26), and solar wind input energy (see Figure 4.27) are higher during the descending than the ascending phase of the solar cycle, except during 24^{th} solar cycle which is still incomplete.

Table 4.6: Data for SN, SWS, SW DynP, SWε, DST index, Kp index, Ap index, and during ascending phases of 14th up to the middle of the 24th solar cycle.

SC (Year)	SN	DST index	KP index	AP index	SW speed	SW Pdyn	SW ε (E+18)	No. of EQ	No. of EQ
14 (1901-1905)	229.5	-	-	-	-	-	-	-	5
15 (1913-1917)	366.1	-	-	-	-	-	-	-	9
16 (1923-1927)	332.8	-	-	-	-	-	-	-	41
17 (1933-1937)	407.4	-	-	-	-	-	-	-	42
18 (1944-1947)	440.4	-	-	-	-	-	-	-	24
19 (1954-1957)	530.8	-	-	-	-	-	-	-	129
20 (1964-1968)	386.7	-	-	-	-	-	-	-	165
21 (1976-1979)	408.8	-68.6	93.3	56.2	1618.8	8.4	1.8	1447	574
22 (1986-1989)	382.8	-77.1	92.5	55.6	1212.9	6.7	2.0	2471	680
23 (1996-2000)	439.0	-74.6	100.9	57.2	2123.8	10.1	2.5	5849	685
24 (2008-2012)	199.2	-39.7	67.9	33.4	2048.0	7.1	1.4	8415	1148

Table 4.7: Data for SN, SWS, SW DynP, SWε, DST index, Kp index, Ap index, and EQ during descending phases of 14th up to the middle of the 24th solar cycle.

SC (Year)	SN	DST index	KP index	AP index	SW Speed	SW Pdyn	SW ε (E+18)	No. of EQ	No. of EQ
14 (1905-1913)	501.3	-	-	-	-	-	-	-	17
15 (1917-1923)	553.5	-	-	-	-	-	-	-	37
16 (1927-1933)	474.9	-	-	-	-	-	-	-	45
17 (1937-1944)	807.4	-	-	-	-	-	-	-	62
18 (1947-1954)	887.3	-	-	-	-	-	-	-	270
19 (1957-1964)	1099.8	-	-	-	-	-	-	-	279
20 (1968-1976)	783.6	-	-	-	-	-	-	-	840
21 (1979-1986)	987.2	-141.3	203.6	127.8	2770.1	14.67	4.9	4181	1281
22 (1989-1996)	896.9	-168.4	201.5	130.6	2676.2	15.06	4.5	6295	1075
23 (2000-2008)	759.8	-136.0	187.0	112.6	4100.8	16.71	5.3	14748	1429
24 (2012-2015)	361.5	-37.9	69.1	36.6	1641.0	6.61	1.9	5169	614

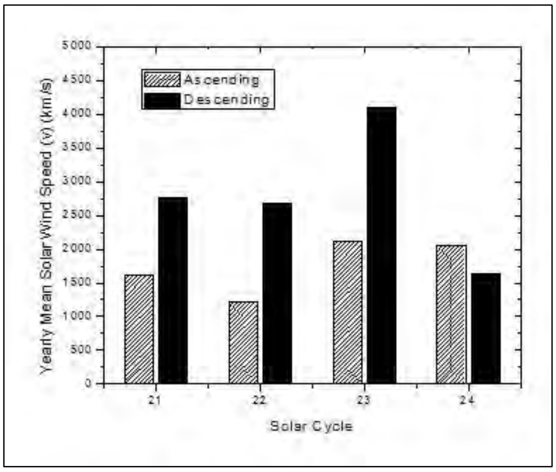

Figure 4.25: The variation of solar wind speed during ascending and descending of 21st up to middle of 24th solar cycle.

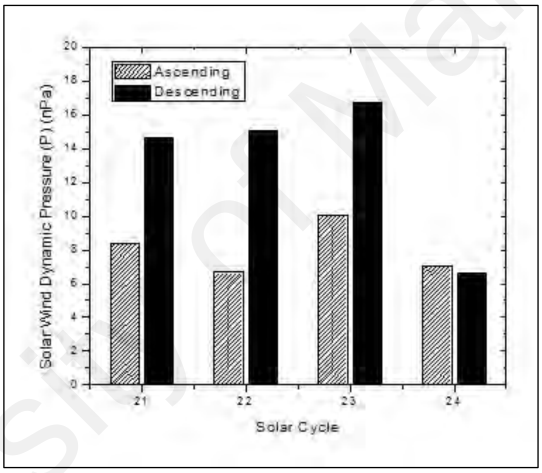

Figure 4.26: The variation of solar wind dynamic pressure during ascending and descending of 21st up to the middle of the 24th solar cycle.

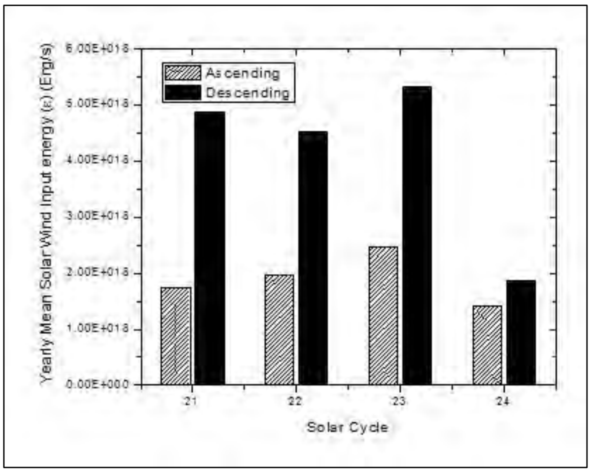

Figure 4.27: The variation of solar wind input energy during ascending and descending of 21st up to the middle of the 24th solar cycle.

Secondly, in order to investigate the inclusion of geomagnetic storm as a mediator to study the correlation between solar and earth seismic activities, we also plotted and examined the graphs of the variation in yearly mean geomagnetic storm indices. We also presented their variation based on ascending and descending phases of the solar cycle. From our investigation, we found that yearly mean DST index (see Figure 4.28), yearly mean Kp index (see Figure 4.29), and yearly mean Ap index (see Figure 4.30) are higher during the descending phase of each of the 21st up to the middle of the 24th solar cycle.

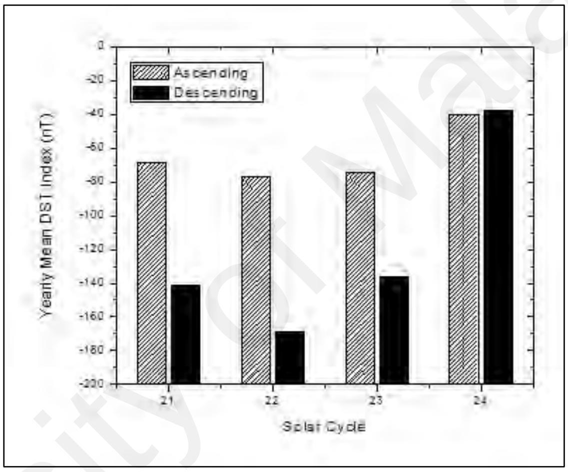

Figure 4.28: The variation of DST index during ascending and descending of 21st up to middle of 24th solar cycle.

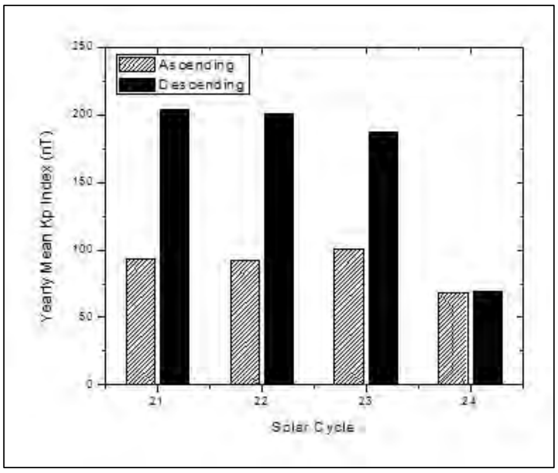

Figure 4.29: The variation of Kp index during ascending and descending of 21st up to middle of 24th solar cycle.

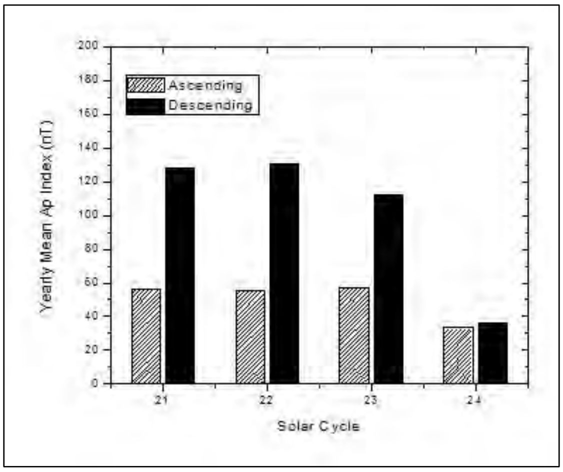

Figure 4.30: The variation of Ap index during ascending and descending of 21st up to middle of 24th solar cycle.

As mentioned before, the solar wind parameters and geomagnetic storm indices were used as a mediator in order to study the correlation between solar and earth seismic activities. From graphs that are presented in Figures 4.25 until 4.30, we concluded that during the 21st up to the middle of the 24th solar cycle, the variation of solar wind parameters and geomagnetic storm indices are higher during the descending phase, except during the incomplete of the 24th solar cycle. In this case, we are motivated to investigate the variation of the annual number of earthquakes during the ascending and descending phases of the solar cycle.

Data of annual numbers of small magnitude earthquakes during the ascending and descending phases that were presented in Tables 4.5 and 4.6 were only available for about ±4 solar cycles only (21st up to middle of 24th solar cycle), while the data of the annual numbers of large magnitude earthquake available about ±11 solar cycles (14th up to middle of 24th solar cycle). Therefore, we plotted and investigated their variation during the ascending and descending phases in different solar cycles. From this research, we found that the variation of the annual number of small (see Figure 4.31) and large magnitude earthquakes (see Figure 4.32) are also higher during the descending phase of the solar cycle, except during the incomplete of the 24th solar cycle.

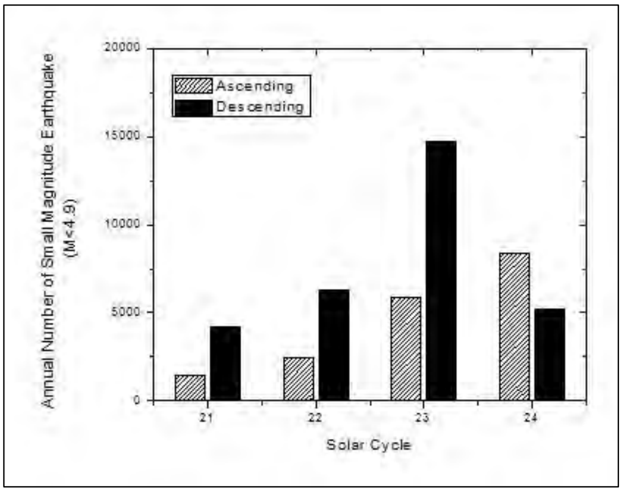

Figure 4.31: The variation of number of small magnitude earthquake during ascending and descending phase of 21st up to middle of 24th solar cycle.

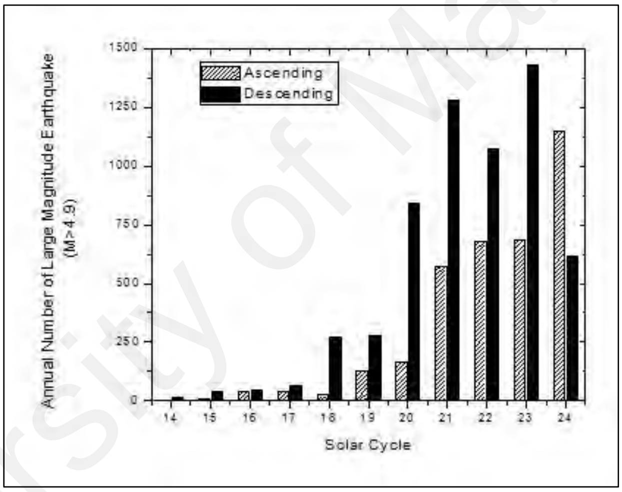

Figure 4.32: The variation of number of large magnitude earthquake during ascending and descending phase of 21st up to middle of 24th solar cycle.

From this section (section 4.2.3), we found that the solar wind parameters, geomagnetic storm indices and the annual number of the earthquake are higher during the descending phase for all solar cycles, except during the incomplete 24th solar cycle. Furthermore, we are motivated to predict the data for the annual number of small and large magnitude earthquakes during the incomplete descending phase of the 24th solar cycle, in order to assist us in investigating their variation during the ascending and descending phase of the 24th solar cycle (from the year 2008 until 2019).

4.2.4 The Prediction of the Data of Annual Number of Earthquakes during the Incomplete Descending Phase of the 24th Solar Cycle

This research predicts the data of an annual number of earthquakes by using two methods of solar cycles, which are based on the yearly mean sunspot number (conventional solar cycle) and the yearly mean solar wind input energy (modified solar cycle) (see Figure 4.33). In this research, data for the annual number of small earthquakes was only available starting from the year 1976 until 2015, which covered the 21st up to the middle of the 24th solar cycle. Hence, we used a polynomial fitting line starting from the 21st until the 23rd solar cycle, to predict the data of the annual number of earthquakes (within next three years (2017-2019)[1]) during the incomplete descending phase of the 24th solar cycle.

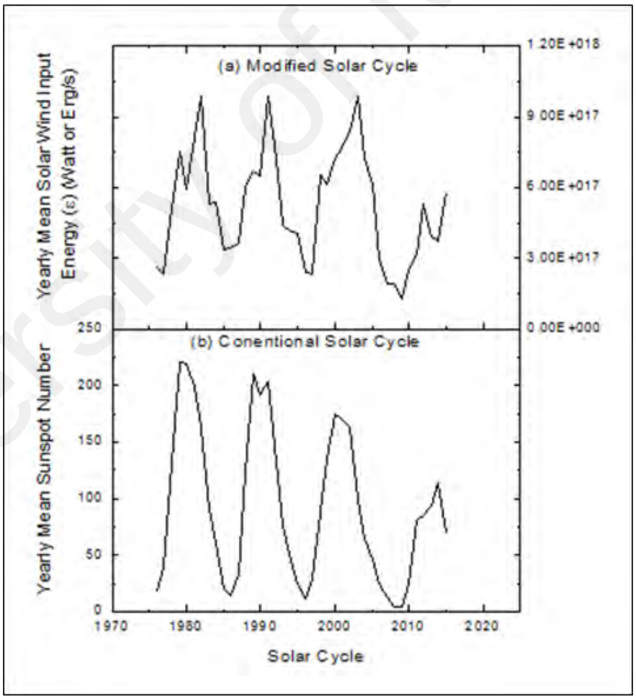

Figure 4.33 : The variation of conventional and modified of 21st up to the middle of the 24th solar cycle.

---

[1] The annual number of small and large earthquake in 2016 retrieved from USGS on 20th January 2017.

4.2.4.1 The prediction by considering the variation of yearly mean sunspot number

The descending phase of the 24th solar cycle was predicted from about 2012 until 2019 (Ajabshirizadeh et al., 2011; Attia et al., 2013; Pesnell, 2008; Pishkalo, 2014; Schatten, 2003). In this section, data for the small and large magnitude earthquakes were predicted by considering the conventional solar cycle. The variation of yearly mean sunspot number was used to indicate the variation of the solar cycle (conventional solar cycle).

Firstly, we focused on predicting the data of an annual number of small magnitude earthquake during the incomplete descending phase of the 24th solar cycle. We plotted the graph of the variation of small magnitude earthquake during the descending phase of the 21st until 23rd solar cycle (see Figures 4.34(a) until 4.34(c)). From those figures, we used the averaged polynomial fitting parameters in order to predict data of the annual number of small magnitude earthquakes during the descending phase of the 24th solar cycle (see Figure 4.34(d)).

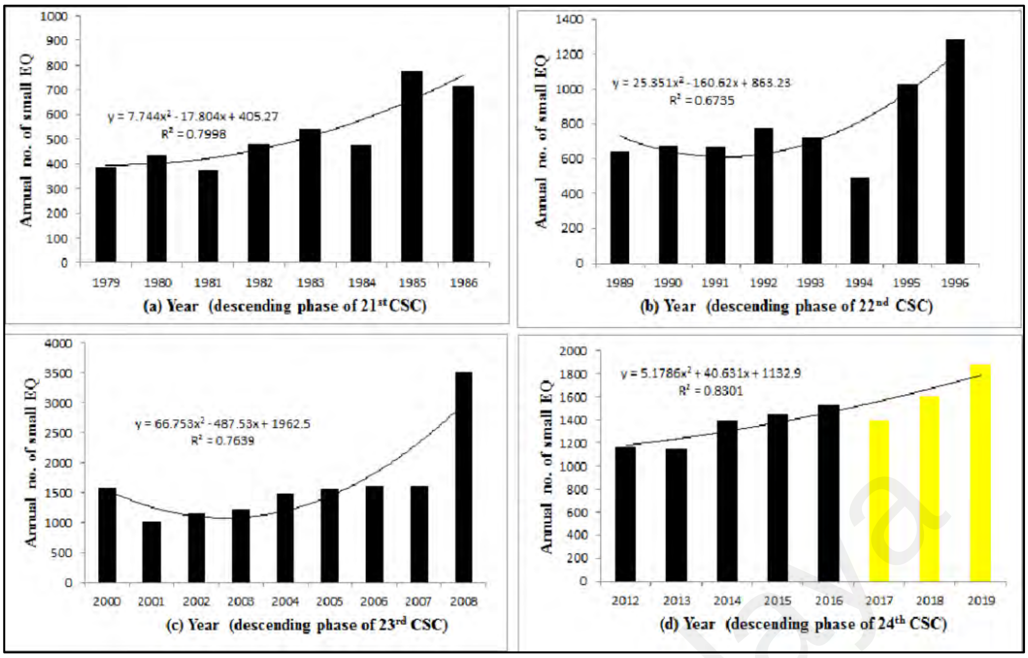

Figure 4.34: The trend of annual small magnitude earthquake (a) during the 21st conventional solar cycle, (b) during the 22nd conventional solar cycle, (c) during the 23rd conventional solar cycle and (d) during prediction of the 24th conventional solar cycle.

Secondly, we predicted the data of large magnitude earthquakes during the incomplete descending phase of the 24th solar cycle. We used the same method with the prediction of an annual number of small magnitude earthquakes. Hence, from the averaged polynomial fitting parameters of the variation in annual number of large magnitude earthquakes during the descending phase of the 21st until 23rd solar cycle (see Figure 4.35(a) until 4.35(c)), we predicted the data for the annual number of large magnitude earthquakes during the descending phase of the 24th solar cycle which is illustrated in Figure 4.35(d).

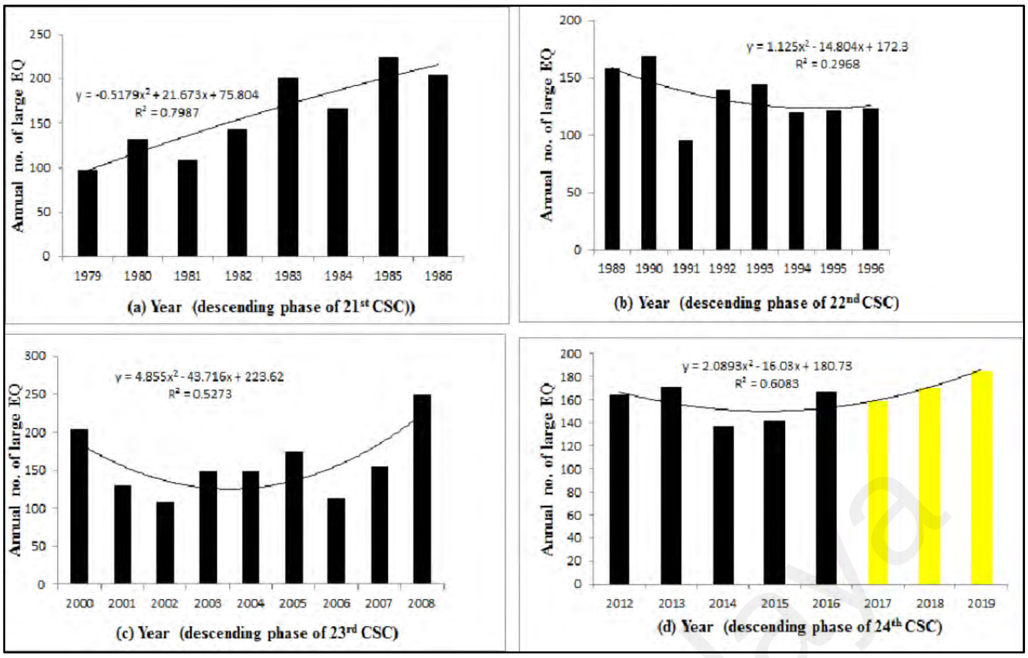

Figure 4.35: The trend of annual large magnitude earthquake (a) during the 21st conventional solar cycle, (b) during the 22nd conventional solar cycle, (c) during the 23rd conventional solar cycle and (d) during prediction of the 24th conventional solar cycle.

4.2.4.2 The prediction by considering the variation of the yearly mean solar wind input energy

Basically, this section uses the same method with the previous section (section 4.2.4.1). We also used the averaged polynomial fitting parameters during descending phase of the 21st until the 23rd solar cycle in order to predict the annual number of small magnitude earthquake during the descending phase of the 24th solar cycle. However, in this section, we used the variation of yearly mean solar wind input energy in order to suggest the modified solar cycle.

For further investigation, firstly, we focused on predicting the data of the annual number of small magnitude earthquakes during the incomplete descending phase of the 24th modified solar cycle. Figures 4.36(a) until 4.36(c) illustrates the variation of small magnitude earthquake during the descending phase of the 21st until 23rd modified solar cycle.

By applying the averaged polynomial fitting parameters of those figures, we predicted the data for the annual number of small magnitude earthquakes during the descending of 24th modified solar cycle (see Figure 4.36(d)).

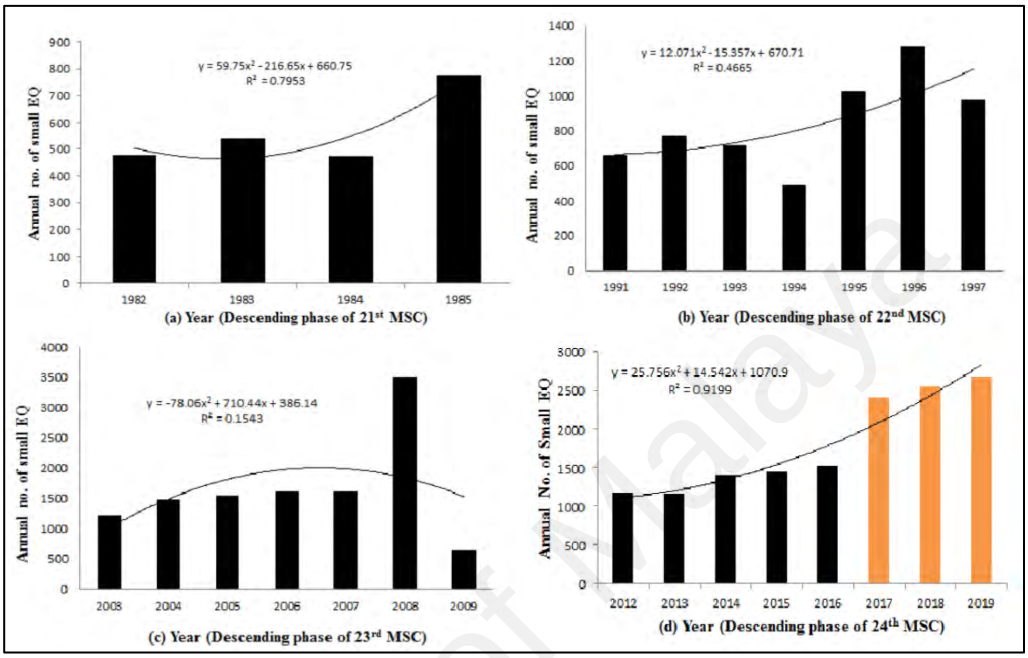

Figure 4.36: The trend of annual small magnitude earthquake (a) during 21st modified solar cycle, (b) during 22nd modified solar cycle, (c) during 23rd modified solar cycle and (d) during prediction of 24th modified solar cycle.

Secondly, we predicted the data of the annual number of large magnitude earthquakes during the incomplete descending phase of the 24th modified solar cycle (see Figure 4.37(d)). This prediction also used the polynomial fitting parameters of the variation large magnitude earthquake during the descending phase of the 21st until 23rd modified solar cycle (see Figure 4.37(a) until 4.37(c)).

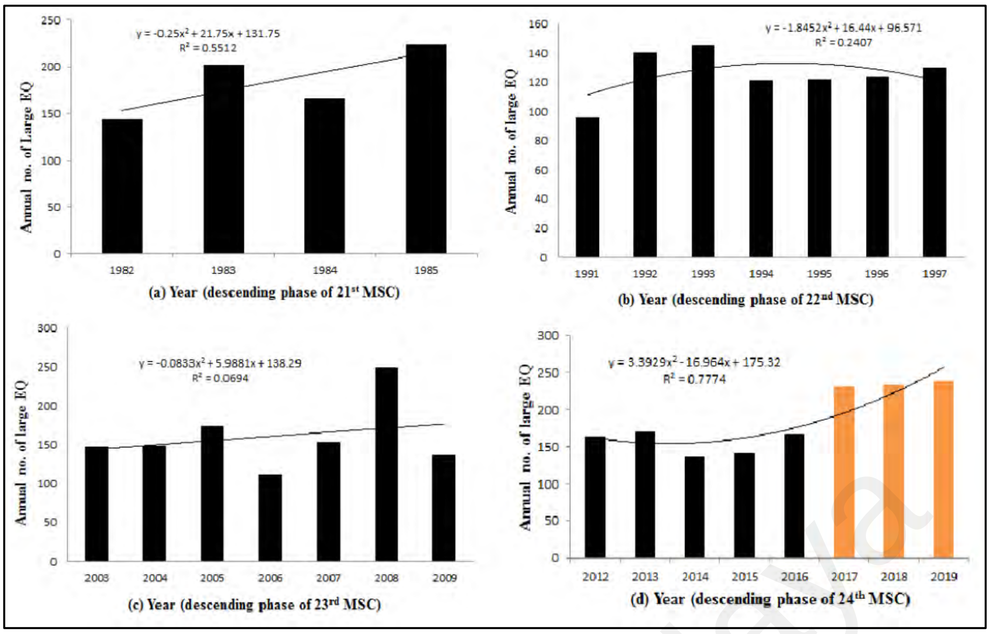

Figure 4.37: The trend of annual large magnitude earthquake (a) during 21st modified solar cycle, (b) during 22nd modified solar cycle, (c) during 23rd modified solar cycle and (d) during prediction of 24th modified solar cycle.

From Figures 4.34 until 4.37, we found that there is an increasing in an annual number of small and large magnitude earthquakes during the descending phase of the 21st until 24th conventional and modified solar cycles. From those figures, we also found that the prediction by considering the variation of the conventional and modified solar cycle, data for the annual small and large magnitude earthquakes for the year 2017 until 2019 increases. From Figures 4.34(d) and 4.36(d), by using the conventional solar cycle, there will be 1395, 1606 and 1883 small magnitude earthquakes annually; and by using the modified solar cycle, there will be 2417, 2550 and 2680 small magnitude earthquakes annually in the year 2017, 2018 and 2019, respectively. As illustrated in Figures 4.34(d) and 4.37(d), by using the conventional solar cycle, there will be 159, 170 and 185 large magnitude earthquakes annually; and by using modified solar cycle, there will be 231, 234 and 238 large magnitude earthquakes annually in the year 2017, 2018 and 2019, respectively.

All the data prediction during the incomplete descending phase of the 24th conventional and modified solar cycle which covers from 2017 until 2019 were presented in Table 4.8. From that Table, we suggested that there is an increasing of the annual number of small and large magnitude earthquake which predicted by using conventional and modified solar cycle's polynomial fitting.

Table 4.8: Data prediction of earthquake during descending phase of 24th solar.

Year	**Annual No. of prediction small EQ (M<4.9)**		**Annual No. of prediction Large EQ (M>4.9)**	
	By CSC	By MSC	By MSC	By MSC
2017	1395	2417	159	231
2018	1606	2550	170	234
2019	1883	2680	185	238

Lastly, we compared the different variation of the data prediction for number of earthquake (2017-2019) between the conventional and modified solar cycles. By referring Figures 4.34 (d) and 4.36 (d), the different variation of the data prediction of the small earthquake was presented in Figure 4.38 (a). Furthermore, by referring Figures 4.35 (d) and 4.37 (d), we also presented the different variation data of the number of large magnitude earthquake (see Figure 3.38 (b)). The yellow bars illustrated in Figure 4.38 are indicate as the data prediction earthquake during 24th conventional solar cycle, while the orange bars are indicate as the data prediction of earthquake during 24th modified solar cycle.

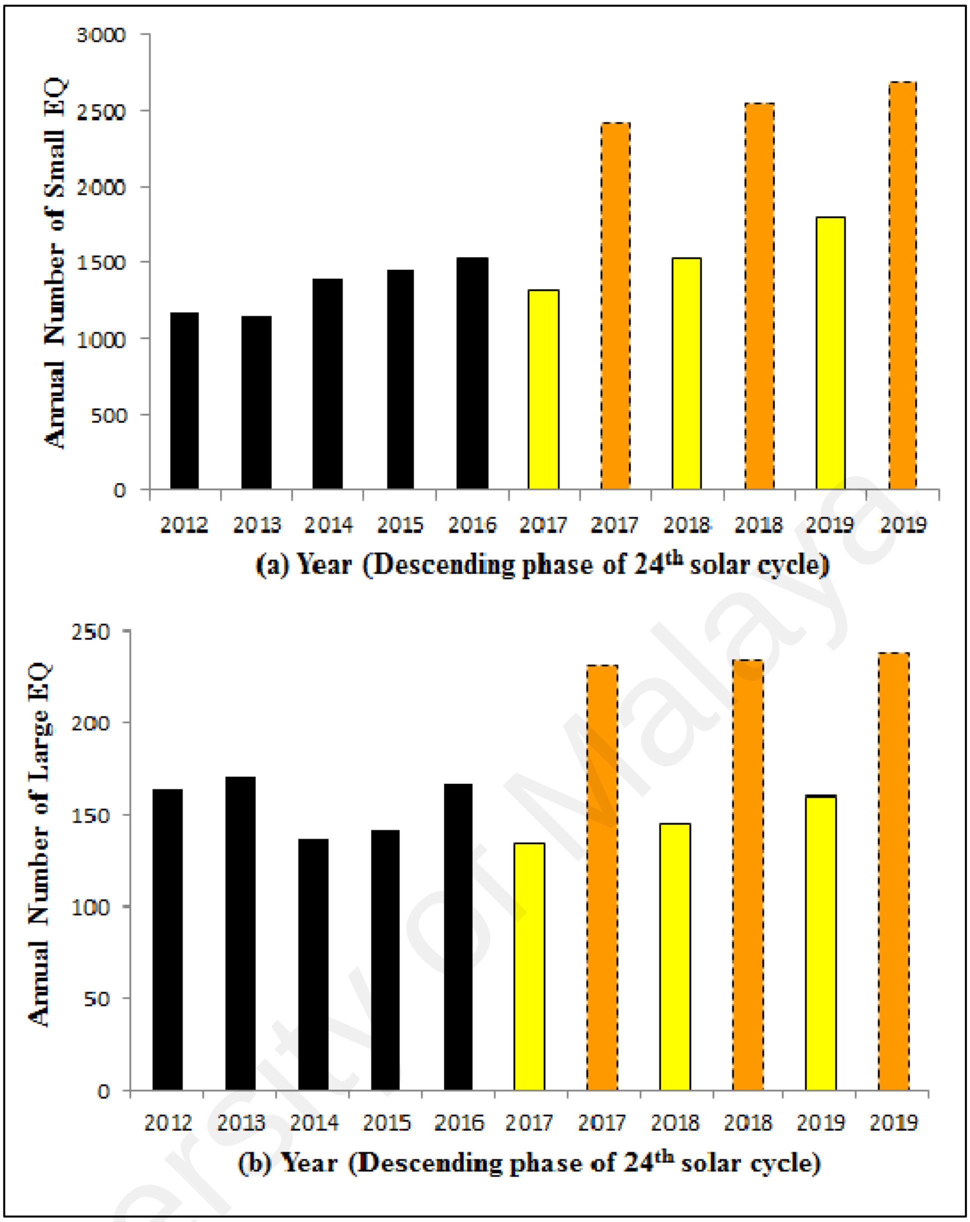

Figure 4.38: The variation of (a) small magnitude earthquake and (b) large magnitude earthquake during 24th solar cycle.

CHAPTER 5: DISCUSSION

From chapter 4, we have investigated and analysed the variation and correlation between the solar and seismic activities by considering the ascending and descending phases of the solar cycles. From the result and analysis of this research, it shows that in each solar cycle, the annual number of small and large magnitude earthquakes were at maximum value during the years of the descending phase. This research also finds that the annual variations of small and large magnitude earthquakes are higher during the descending phase. By implementing the solar wind parameters and geomagnetic storm indices, this research used those two data sets in order to explain the physical mechanism of solar and seismic activities. Other than that, several topics such as the Lorentz force, the interaction between solar wind and earth magnetic field, and energetic particles driven into the magnetosphere layer are also involved in order to discuss the physical mechanism of solar activities and its influence on earthquake occurrences.

5.1 Lorentz Force

The Lorentz force is the total electric and magnetic field forces exerted on an electrically charged particle in an electromagnetic field (Montalibet et al., 2001). The ocean's ability to induce electromagnetic fields from the movement of seawater relies on the deflection of electrically charged sea water ions by the Lorentz force perpendicular to the velocity and magnetic field vectors (Tyler et al., 2003):

$$\boldsymbol{F\ Lorentz} = \boldsymbol{q}[\boldsymbol{E} + (\boldsymbol{V} \times \boldsymbol{B})] \qquad (4)$$

where q is the charge of the water ions, v is their velocity and E and B are the electric and magnetic fields, respectively.

This research involves the use of the Lorentz force as a geophysical aspect in order to explain the piezo magnetic effect. (Sasai (1980),(1984)) investigated the tectonic magnetic field based on the linear piezo magnetic effect and mentioned that the magnetic field changes due to stress force. This force is an indication of the effect on the magnetized earth's crust and upper mantle due to the underground telluric currents. The influence of the Lorentz force concept in the process of the tectonic stress and seismic activities has been studied by Duma and Ruzhin (2003). They suggested that the Lorentz force results from the interaction between magnetic field of the earth and lithosphere, where from their interaction induced the sq-variation currents. The sq-variation can be investigated with different local case area and time. Rabeh et al. (2010) investigated the diurnal and long-term Sq-variation with seismic activities for an area in the Sinai Peninsula. Their results showed that there is a good correlation between the Sq-variation with seismic activity.

Other than that, Duma and Ruzhin (2003) investigated the Sq-variation with earthquake for the E-China region and they also found the earthquake distribution follows the Sq-variation. Therefore, the interactions between the induced Sq-variation current in the earth's lithosphere and earth's magnetic field were considered as the mechanism of that possibly influences the process of the tectonic stress field and seismic activities.

5.2 Solar Wind and Earth Magnetic Field Interaction

As mentioned before, the interaction between solar wind and earth magnetic field may assist us in understanding the mechanism of the correlation between solar and seismic activities. The interaction between solar wind parameters and geomagnetic activities, and their contributions in the process of the tectonic plate movement are called as the solar geo-dynamo process. Therefore, this research considers the interaction between the solar wind parameters with the earth's magnetic field (geomagnetic storm activities) and how it may affects the movements of the tectonic plates, which can lead to the occurrence of earthquake.

In addition, Rusov et al. (2010) proposed the mechanism of "solar dynamo-geodynamo" connection by studying the correlation between energy in the Sun's core layer and the earth's magnetic field. They proposed that the energy initially is modulated by the magnetic field of the solar tachocline zone and is consequently absorbed in the Earth's liquid core layer under the influence of terrestrial magnetic field. They concluded that the Sun's core layer is playing the role of the energy source and acts as a modulator of the earth's magnetic field. Therefore, in our research, we found that the geomagnetic storm indices variation follows the variation of the solar wind parameters in every solar cycle, whereas the solar wind parameters and geomagnetic storm indices maximum values were found during descending phase of the solar cycle (see Chapter 4). In other words, the variation between solar wind parameters and geomagnetic indices show a positive correlation. This result agrees to the previous studies by Pellinen et al. (1982), where they mentioned that the substorm activity (AE and AL indices) over the Scandinavia region correlated with to solar wind input energy. The variation of geomagnetic storm index produced during descending phase of the solar cycle also agrees with Mansilla (2014). Le et al. (2013) investigated the variation of DST index by considering ascending and descending phases of the solar cycle. Their conclusion supports our finding of geomagnetic storm indices at maxima and higher during descending phase.

By taking into account of the explanation of the Lorentz force and the mechanism of the "solar dynamo and geodynamo" connection, it can be concluded that the variation in the energy of the sun is the main source of the earth's magnetic field which is affecting the geomagnetic storm activities (DST, Kp and Ap indices). On the other hand, the interaction between the sq-variation in the earth magnetic field and lithosphere layer have considerable influence on the tectonic plate movement and seismic activity. Therefore, this research also finds that the maximum values of the annual number for small and large magnitude earthquakes were during the descending phase of the solar cycle, whereas the maximum value of the geomagnetic storm activities which results from the interaction of the solar wind and magnetic field of the earth also found during the descending phase of the solar cycle.

The results of our research were agreed and supported by several previous researchers. For example, Florindo and Alfonsi (1995) and Florindo et al. (1996) investigated and examined the variation of strong earthquakes ($M \geq 7$) correlated to the sudden change of the earth's magnetic field. They proposed and assumed that the earthquake occurrences react upon the geodynamo at the Core Mantle Boundary, thus causing the changes in the geomagnetic storm activity.

Other than that, Duma and Vilardo (1998) investigated the variation of the earthquakes activities with magnitude not exceeding 3.4 (small earthquake) during 1972 – 1996 in the Mt. Vesuvius area and their correlation to the solar activity (solar flux) and earth's magnetic field. They concluded that the variation of the solar activity and the earth's magnetic field correlates to the variation of earthquake occurrences. Hence, from their study, our research assumes that by studying the correlation between solar activities (by investigating the variation sunspot number and solar wind parameters) and earth's magnetic field (by studying the geomagnetic storm indices), likewise the earth's magnetic field interacts with the lithosphere layer can be used in order to explain and investigate the relationship between the solar and seismic activities. Other than that, our research also agrees with Thébault et al. (2010). They studied on the magnetic field of the lithosphere, which is bounded at depth by mineralogical changes and elevated temperatures. From their research, they assumed that the magnetic crust can be related to tectonic and thermal processes.

5.3 Energetic Mass Particles of the Solar Wind

As mentioned in Chapter 2, the solar cycles are divided into 4 phases; ascending, maxima, descending and minima. However, in Chapter 4, it has been shown that the annual number of small and large earthquakes for China and its bordering countries are higher during the descending phase. Therefore, this research also explains the possible factors influencing earthquake occurrences during that phase by interpreting the solar energy transfers into the earth magnetosphere layer.

In addition, other possible activities of the Sun that are involved in the interaction between the solar wind and earth magnetosphere layer also included in this discussion. Lopez et al. (2004) mentioned that the solar wind is the prime source of energy transfer into the magnetosphere layer. They suggested that quantifying the energy transfer from the solar wind into the magnetosphere layer is a fundamental problem in space physics. Ballatore (2002) studies the Sun-Earth relation by considering the interaction between the interplanetary medium and the terrestrial magnetosphere. He proposed that the energy and particles of the Sun can enter the magnetosphere when reconnection occurs between interplanetary magnetic field (IMF) and geomagnetic field. Augusto et al. (2012) also mentioned that during the 11 year of solar cycle, the earth's space environment varies. It is disturbed by coronal mass ejection and corotating interaction region from corona layer.

Moreover, there are other solar activities that participate in the transfer of solar wind energy into the magnetosphere layer, namely; coronal mass ejection (CME) and corrotating index rotation (CIR). In other words, the variation and correlation between the solar wind parameters and geomagnetic storm indices were based on the activities of the CME and CIR from corona holes (Xiao-Fei et al., 2015). On the other hand, the activities of the CMEs and CIRs are varied by solar cycles. As mentioned in Chapter 2, in each solar cycle, the maximum activity of the CME is during solar maxima, while CIR is during descending phase of the solar cycle (Ballatore, 2002; Guarnieri et al., 2006; Kivelson & Russell, 1995; Richardson & Cane, 2012; Richardson et al., 2000). The variation of CME and CIR are illustrated in Figure 5.1.

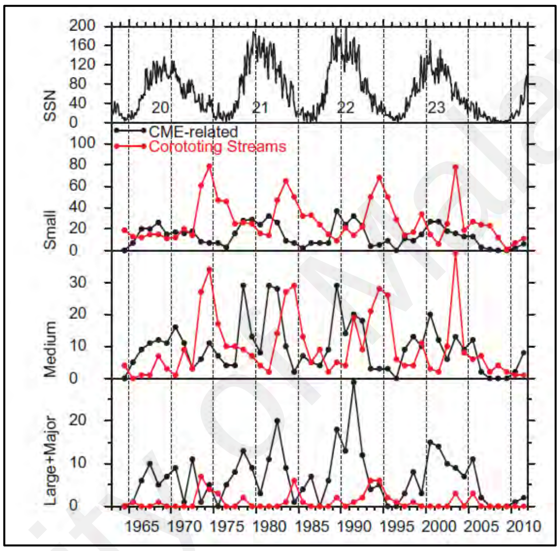

Figure 5.1: The variation of large + major, medium and small geomagnetic storms in 1964 – 2011 (during 20th up to 23rd solar cycle) associated with CME and CIR(Richardson & Cane, 2012).

Richardson and Cane (2012) investigated the variation of geomagnetic indices and their correlation with the CME and CIR during the 20th up to the 23rd solar cycles. From their research, they found out that, in every solar cycle variation, the CME activities follow the variation of sunspot number (solar cycle), while CIR activities are typically prominent during the descending phase. Hence, by referring to Figure 5.1, we concluded that the maximum value of solar wind parameters (see Figures 4.2 to 4.5) and geomagnetic storm indices (see Figures 4.6 to 4.9) during the descending phase are due to the activities of CIRs prominent on that phase. Therefore, we also found out that the maximum value of annual small magnitude earthquakes during the descending phase (see Figures 4.10 to 4.13). The maximum value of large magnitude earthquakes from the 14th up to middle of 24th solar cycle are also found during the descending phase, except for the 22nd solar cycle (see Figures 4.14 to 4.24). During 22nd solar cycle, the maximum value of large magnitude earthquake occurs near to solar maxima due to CME activity.

In addition, the highest activity of the CMEs and CIRs are at maxima and during the descending phase of the solar cycle, likewise the descending phase is longer than ascending phase (Khain & Khalilov, 2007). Therefore, as shown in Chapter 4, we found that the variation of solar wind parameters and geomagnetic storm indices are higher during the descending phase (see Figures 4.25 to 4.30). Therefore, we also found out that the variation of small and large magnitude earthquakes are higher during the descending phase (see Figures 4.31 to 4.32).

CHAPTER 6: CONCLUSION AND FUTURE WORK

This research was designed to investigate the correlation between solar and seismic activities by interpreting the solar wind and geomagnetic storm parameters to understand the physical phenomena. In the case of the solar wind, we investigated the variation of speed, dynamic pressure and input energy of the solar wind. For the geomagnetic storm phenomena, we looked at the variation of the DST, Kp and Ap indices. All these aspects are divided and investigated by considering the ascending and descending phases of each solar cycle.

The investigation on the maximum value of the solar wind parameters (speed, dynamic pressure and input energy of the solar wind) and geomagnetic storm activities (DST, Kp and Ap indices) during the year of the descending phase of each solar cycle has shown that the geomagnetic activities are related to the solar wind activities. It has also shown that the maximum value of the annual number of small and large magnitude earthquakes is found during the years of the descending phase. These finding suggests that in general, the increment and maximum value of earthquakes during the descending phase is triggered by maximum value/activity of the solar wind and geomagnetic storm during that phase.

The most obvious finding to emerge from this research is that by considering the ascending and descending phases of each solar cycle, we found that the solar wind parameters and geomagnetic storm indices are higher during the descending phase of the solar cycle. On the other hand, the annual numbers of small and large magnitude earthquakes are also found to be higher during the descending phase. The result of this investigation shows that the increment of the earthquake occurrence during the descending phase is triggered by the higher activity of the solar wind and geomagnetic storm during that phase.

By considering the implementation of the polynomial fitting line of the conventional solar cycle (sunspot number variation) and modified solar cycle (solar wind input energy variation), the annual numbers of small magnitude earthquakes during the incomplete descending phase of 24th solar cycle were predicted. It is suggested there will be significantly higher number of annual small and large magnitude earthquakes within the next three years until 2019.

As a result of this, the maximum value of earthquake occurrences is during the descending phase of the solar cycle, and our research seems to support the link with the increase in geomagnetic and solar wind activities during that phase. The result of this research supports the idea of the corona rotating streams increasing during the descending phase of the solar cycle, while the speed of the solar wind is based on the activities of the CME and corona rotating streams. On the other hand, the suggested implication of this research is that the higher values of geomagnetic indices are proportional to the higher value of solar wind energy transferred to the magnetosphere layer. Hence, we concluded that the increasing of the earthquake occurrences during descending phase of the solar cycle was triggered by the increment of interaction between solar wind and earth magnetic field.

The finding from this research makes several contributions to the current literature. Firstly, the solar physics subject can be used in order to study the geophysical phenomena. Secondly, the inclusion of geomagnetism phenomena may assist us in understanding how the solar activities penetrate the magnetosphere layer. Thirdly, the energy penetration of the solar activity into earth's core layer through interaction between the solar wind and earth's magnetic field may assist us to understand and investigate the correlation between solar and seismic activities.

As the act of solar cycle varies and the occurrences of earthquakes can be happened in different latitudes and longitudes, further research should be done in order to investigate the variation of the earthquakes in different case study areas and magnitudes. Future studies on the next ascending and descending phases of the solar cycle (i.e 25^{th} solar cycle) are therefore recommended.

Overall, this research achieves all the objectives mentioned at the beginning of this research (see section 1.3).

REFERENCES

Adebesin, B., Ikubanni, S., Kayode, J., & Adekoya, B. (2013). Variability of solar wind dynamic pressure with solar wind parameters during intense and severe storms. *The African Review of Physics, 8*, 119-128.

Ajabshirizadeh, A., Jouzdani, N. M., & Abbassi, S. (2011). Neural network prediction of solar cycle 24. *Research in Astronomy and Astrophysics, 11*(4), 491-496.

Akasofu, S.-I. (1981). Energy coupling between the solar wind and the magnetosphere. *Space Science Reviews, 28*(2), 121-190.

Akasofu, S.-I., & Chapman, S. (1972). *Solar-terrestrial physics*. Oxford, England: Clarendon Press.

Anagnostopoulos, G., & Papandreou, A. (2012). Space conditions during a month of a sequence of six M> 6.8 earthquakes ending with the tsunami of 26 December 2004. *Natural Hazards and Earth System Sciences, 12*(5), 1551–1559.

Arge, C. N., Odstrcil, D., Pizzo, V. J., Mayer, L. R., Velli, M., Bruno, R., & Malara, F. (2003). *Improved method for specifying solar wind speed near the Sun.* Paper presented at the AIP Conference Proceedings, Pisa, Italy: American Institute of Physics.

Attia, A.-F., Ismail, H. A., & Basurah, H. M. (2013). A Neuro-Fuzzy modeling for prediction of solar cycles 24 and 25. *Astrophysics and Space Science, 344*(1), 5-11.

Augusto, C., Kopenkin, V., Navia, C., Tsui, K., Shigueoka, H., Fauth, A., . . . Miranda, P. (2012). Variations of the muon flux at sea level associated with interplanetary icmes and corotating interaction regions. *The Astrophysical Journal, 759*(2), 143.

Ballatore, P. (2002). Effects of fast and slow solar wind on the correlations between interplanetary medium and geomagnetic activity. *Journal of Geophysical Research: Space Physics, 107*(A9).

Bartels, J. (1932). Terrestrial-magnetic activity and its relations to solar phenomena. *Terrestrial Magnetism and Atmospheric Electricity, 37*(1), 1-52.

Benjamin, A. D., & Nayar, S. (2010). Characteristics of interplanetary CMEs observed by Ulysses. *Indian Journal of Radio & Space Science, 39*, 270-275.

Biktash, L. (2012). Statistical study of solar wind parameters and evolution of dst variations during 19-23 solar cycles in relation with cosmic ray variations. *Sun and Geosphere, 7*, 41-44.

Brandt, P., Schmidt, W., & Steinegger, M. (1990). On the umbra-penumbra area ratio of sunspots. *Solar Physics, 129*(1), 191-194.

Brekke, A. (2012). *Physics of the upper polar atmosphere*. Berlin, Germany: Springer Science & Business Media.

Brummell, N. H., Tobias, S. M., Thomas, J. H., & Weiss, N. O. (2008). Flux pumping and magnetic fields in the outer penumbra of a sunspot. *The Astrophysical Journal, 686*(2), 1454.

Budyko, M. I. (1969). The effect of solar radiation variations on the climate of the earth. *Tellus, 21*(5), 611-619.

Charbonneau, P., Dalsgaard, J. C., Henning, R., Larsen, R. M., Schou, J., Thompson, M. J., & Tomczyk, S. (1999). Helioseismic constraints on the structure of the solar tachocline. *The Astrophysical Journal, 527*(1), 445.

Chitre, S. (1963). The structure of sunspots. *Monthly Notices of the Royal Astronomical Society, 126*(5), 431-443.

Dalsgaard, J. C., & Thompson, M. J. (2007). Observational results and issues concerning the tachocline. In D. W. Hughes, R. Rosner & N. O. Weiss (Eds.), *Solar Tachocline* (pp. 53-85). Cambridge, England: Cambridge University Press.

Deinzer, W. (1965). On the magneto-hydrostatic theory of sunspots. *The Astrophysical Journal, 141*, 548.

Delamere, P. A. (2015). Solar wind interaction with giant magnetospheres and earth's magnetosphere. In A. Keiling, C. M. Jackman & P. A. Delamere (Eds.), *Magnetotails in the Solar System* (pp. 217-233). Hoboken, New Jersey: John Wiley & Sons, Inc.

Duma, G., & Ruzhin, Y. (2003). Diurnal changes of earthquake activity and geomagnetic Sq-variations. *Natural Hazards and Earth System Sciences, 3*(3/4), 171-177.

Duma, G., & Vilardo, G. (1998). Seismicity cycles in the Mt. Vesuvius area and their relation to solar flux and the variations of the earth's magnetic field. *Physics and Chemistry of the Earth, 23*(9-10), 927-931.

Dutta, P., Mishra, O., & Naskar, M. (2013). A review of operational earthquake forecasting methodologies using linguistic fuzzy rule-based models from imprecise data with weighted regression approach. *Journal of Sustainability Science and Management, 8*(2), 220-235.

Elliott, J., & Gough, D. (1999). Calibration of the thickness of the solar tachocline. *The Astrophysical Journal, 516*(1), 475.

Florindo, F., & Alfonsi, L. (1995). Strong earthquakes and geomagnetic jerks: a cause-effect relationship? *Annals of Geophysics, 38*(3-4), 457–461.

Florindo, F., Alfonsi, L., Piersanti, A., Spada, G., & Marzocchi, W. (1996). Geomagnetic jerks and seismic activity. *Annali di Geofisica, 39*, 1227-1233.

Gnevyshev, M. (1967). On the 11-years cycle of solar activity. *Solar Physics, 1*(1), 107-120.

Gonzalez, W., Joselyn, J., Kamide, Y., Kroehl, H., Rostoker, G., Tsurutani, B., & Vasyliunas, V. (1994). What is a geomagnetic storm? *Journal of Geophysical Research: Space Physics, 99*(A4), 5771-5792.

Gosling, J. (1996). Corotating and transient solar wind flows in three dimensions. *Annual Review of Astronomy and Astrophysics, 34*(1), 35-73.

Gosling, J., & Bame, S. (1972). Solar-wind speed variations 1964–1967: An autocorrelation analysis. *Journal of Geophysical Research, 77*(1), 12-26.

Gousheva, M., Georgieva, K., Kirov, B., & Antanasov, D. (2003). *On the relation between solar activity and seismicity*. Paper presented at the Proceedings of the International Conference on Recent Advances in Space Technologies, Istanbul, Turkey: IEEE.

Guarnieri, F. L., Tsurutani, B. T., Gonzalez, W. D., Echer, E., Gonzalez, A. L., Grande, M., & Soraas, F. (2006). *ICME and CIR storms with particular emphasis on HILDCAA events.* Paper presented at the ILWS Workshop, Goa, India: Quest Publications for ILWS and Indian Institute of Geomagnetism.

Gupta, M. D., & Basu, D. (1965). Solar-terrestrial events in relation to the phase of the solar cycle. *Journal of Atmospheric and Terrestrial Physics, 27*(9), 1029-1032.

Howard, R., & LaBonte, B. (1980). The sun is observed to be a torsional oscillator with a period of 11 years. *The Astrophysical Journal, 239*, L33-L36.

Hoyt, D. V., & Schatten, K. H. (1998). Group sunspot numbers: A new solar activity reconstruction. *Solar Physics, 181*(2), 491-491.

Hundhausen, A. J. (1979). Solar activity and the solar wind. *Reviews of Geophysics, 17*(8), 2034-2048.

Hundhausen, A. J. (2012). *Coronal expansion and solar wind*. Berlin, Germany: Springer Science & Business Media.

Hynönen, R. (2013). *Geomagnetic activity and its sources during modern solar maximum.* (Master's Thesis), University Of Helsinki. Retrieved from https://helda.helsinki.fi/handle/10138/42004.

Jankowski, J., & Sucksdorff, C. (1996). *Guide for magnetic measurements and observatory practice*. Boulder, Colorado: International Association of Geomagnetism and Aeronomy Warsaw.

Jusoh, M., Liu, H., Yumoto, K., Uozumi, T., Takla, E., Yousif Suliman, M., . . . Hashim, M. (2012). *Investigation on the Possible Relationship between Magnetic Pulsations and Earthquakes.* Paper presented at the AGU Fall Meeting Abstracts, Boulder, Colorado: American Geophysical Union.

Khain, V., & Khalilov, E. (2007). About possible influence of solar activity upon seismic and volcanic activities: Long-term forecast. *Transactions of the International Academy of Science*, 217-240.

Khodairy, S. S., El Hadidy, M. S., Semeida, M. A., Hamed, R. A., & Youssef, S. A. (2015). Relationship between seismicity and solar activities during solar cycle 22. *International Journal, 3*(2), 9-17.

Kivelson, M. G., & Russell, C. T. (1995). *Introduction to space physics*. Cambridge, United Kingdom: Cambridge University Press.

Koskinen, H. E., & Tanskanen, E. I. (2002). Magnetospheric energy budget and the epsilon parameter. *Journal of Geophysical Research: Space Physics, 107*(A11), SMP 42-41–SMP 42-10.

Kovner, M., & Feldstein, Y. I. (1973). On solar wind interaction with the Earth's magnetosphere. *Planetary and Space Science, 21*(7), 1191-1211.

Krüger, A. (2012). *Introduction to solar radio astronomy and radio physics*. Berlin, Germany: Springer Science & Business Media.

Lang, K. R. (1995). Sun, earth and sky. *Earth, Moon, and Planets, 70*(1), 1-20.

Lang, K. R. (2002). *Latest advances in solar astronomy.* Paper presented at the The evolving sun and its influence on planetary environments, San Francisco: Astronomical Society of the Pacific.

Lanza, R., & Meloni, A. (2006). *The earth's magnetism*. Berlin, Germany: Springer.

Le, G.-M., Cai, Z.-Y., Wang, H.-N., Yin, Z.-Q., & Li, P. (2013). Solar cycle distribution of major geomagnetic storms. *Research in Astronomy and Astrophysics, 13*(6), 739-748.

Lites, B., & Thomas, J. (1985). Sunspot umbral oscillations in the photosphere and low chromosphere. *The Astrophysical Journal, 294*, 682-688.

Loewe, C., & Prölss, G. (1997). Classification and mean behavior of magnetic storms. *Journal of Geophysical Research: Space Physics, 102*(A7), 14209-14213.

Lopez, R., Wiltberger, M., Hernandez, S., & Lyon, J. (2004). Solar wind density control of energy transfer to the magnetosphere. *Geophysical Research Letters, 31*(8).

Lu, H., Jarvis, M. J., & Hibbins, R. E. (2008). Possible solar wind effect on the northern annular mode and northern hemispheric circulation during winter and spring. *Journal of Geophysical Research: Atmospheres, 113*(D23).

Mansilla, G. A. (2014). Solar cycle and seasonal distribution of geomagnetic storms with sudden commencement. *Earth Science Research, 3*(1), 50.

Mayaud, P.-N. (1980). *Derivation, meaning, and use of geomagnetic indices*. Washington, DC: American Geophysical Union Geophysical Monograph Series.

Merrill, R. T., & McElhinny, M. W. (1983). *The earth's magnetic field: Its history, origin and planetary perspective*. London and New York: Academic Press.

Meyer, F. D. (2006). *The geomagnetic aa index as a precursor of solar activity*. Brussels, Belgium: Koninklijk Meteorologisch Instituut.

Midya, S., & Gole, P. (2014). Trend of major earthquakes during the period 1900–2011 and its association with some solar and geomagnetic parameters. *Indian Journal of Physics, 88*(1), 1-4.

Miesch, M. S. (2005). Large-scale dynamics of the convection zone and tachocline. *Living Reviews in Solar Physics, 2*(1), 1-139.

Montalibet, A., Jossinet, J., & Matias, A. (2001). Scanning electric conductivity gradients with ultrasonically-induced Lorentz force. *Ultrasonic Imaging, 23*(2), 117-132.

Motulsky, H. J., & Ransnas, L. A. (1987). Fitting curves to data using nonlinear regression: a practical and nonmathematical review. *The FASEB Journal, 1*(5), 365-374.

Nakano, S., Ueno, G., Ohtani, S., & Higuchi, T. (2009). Impact of the solar wind dynamic pressure on the Region 2 field-aligned currents. *Journal of Geophysical Research: Space Physics, 114*(A2).

Neugebauer, M. (1975). Large-scale and solar-cycle variations of the solar wind. *Space Science Reviews, 17*(2-4), 221-254.

O'Hagan, A., & Kingman, J. (1978). Curve fitting and optimal design for prediction. *Journal of the Royal Statistical Society. Series B (Methodological)*, 1-42.

O'Brien, K. (2007). Cosmic-ray propagation through the disturbed heliosphere. *Acta Astronautica, 60*(4), 541-546.

Odintsov, S., Boyarchuk, K., Georgieva, K., Kirov, B., & Atanasov, D. (2006). Long-period trends in global seismic and geomagnetic activity and their relation to solar activity. *Physics and Chemistry of the Earth, Parts A/B/C, 31*(1), 88-93.

Pellinen, R., Baumjohann, W., Heikkila, W., Sergeev, V., Yahnin, A., Marklund, G., & Melnikov, A. (1982). Event study on pre-substorm phases and their relation to the energy coupling between solar wind and magnetosphere. *Planetary and Space Science, 30*(4), 371-388.

Pesnell, W. D. (2008). Predictions of solar cycle 24. *Solar Physics, 252*(1), 209-220.

Pishkalo, M. I. (2014). Prediction of solar cycle 24 using sunspot number near the cycle minimum. *Solar Physics, 289*(5), 1815-1829.

Pizzo, V. (1978). A three-dimensional model of corotating streams in the solar wind, 1. Theoretical foundations. *Journal of Geophysical Research: Space Physics, 83*(A12), 5563-5572.

Praderie, F., Spicer, D. S., Withbroe, G. L., & Benz, A. O. (1981). *Activity and outer atmospheres of the sun and stars: eleventh advanced course of the swiss society of astronomy and astrophysics*. Sauverny: Observatoire de Genève.

Priestley, M., & Chao, M. (1972). Non-parametric function fitting. *Journal of the Royal Statistical Society. Series B (Methodological)*, 385-392.

Prise, A., Harra, L., Matthews, S., Arridge, C. S., & Achilleos, N. (2015). Analysis of a coronal mass ejection and corotating interaction region as they travel from the Sun passing Venus, Earth, Mars, and Saturn. *Journal of Geophysical Research: Space Physics, 120*(3), 1566-1588.

Pulinets, S., & Boyarchuk, K. (2004). *Ionospheric precursors of earthquakes*. Berlin, Germany: Springer Science & Business Media.

Rabeh, T., Miranda, M., & Hvozdara, M. (2010). Strong earthquakes associated with high amplitude daily geomagnetic variations. *Natural Hazards, 53*(3), 561-574.

Richardson, I. G., & Cane, H. V. (2012). Solar wind drivers of geomagnetic storms during more than four solar cycles. *Journal of Space Weather and Space Climate, 2*, A01.

Richardson, I. G., Cliver, E. W., & Cane, H. V. (2000). Sources of geomagnetic activity over the solar cycle: Relative importance of coronal mass ejections, high-speed streams, and slow solar wind. *Journal of Geophysical Research: Space Physics, 105*(A8), 18203-18213.

Roelof, E. C., & Sibeck, D. G. (1993). Magnetopause shape as a bivariate function of interplanetary magnetic field Bz and solar wind dynamic pressure. *Journal of Geophysical Research: Space Physics, 98*(A12), 21421-21450.

Rostoker, G. (1972). Geomagnetic indices. *Reviews of Geophysics, 10*(4), 935-950.

Rusov, V., Linnik, E., Kudela, K., Mavrodiev, S. C., Zelentsova, T., Smolyar, V., & Merkotan, K. (2010). Solar axions as an energy source and modulator of the Earth magnetic field. *arXiv preprint arXiv:1008.1461*.

Sasai, Y. (1980). Application of the elasticity theory of dislocations to tectonomagnetic modelling. *Bulletin of the Earthquake Research Institute, 55*, 387-447.

Sasai, Y. (1984). A surface integral representation of the tectonomagnetic field based on the linear piezomagnetic effect. *Bulletin of the Earthquake Research Institute, 58*, 763-785.

Schatten, K. (2003). Solar activity and the solar cycle. *Advances in Space Research, 32*(4), 451-460.

Simpson, J. F. (1967). Solar activity as a triggering mechanism for earthquakes. *Earth and Planetary Science Letters, 3*, 417-425.

Smil, V. (2012). *Energy: a beginner's guide*. London, United Kingdom: Oneworld Publications.

Sobolev, G., Zakrzhevskaya, N., & Kharin, E. (2001). On the relation between seismicity and magnetic storms. *Izvestiya, Physics of the Solid Earth, 37*(11), 917-927.

Solomon, S. C., Woods, T. N., Didkovsky, L. V., Emmert, J. T., & Qian, L. (2010). Anomalously low solar extreme-ultraviolet irradiance and thermospheric density during solar minimum. *Geophysical Research Letters, 37*(16).

Song, W.-b., Wang, J.-x., & Ma, X. (2005). A study of the north-south asymmetry of solar photospheric magnetic flux. *Chinese Astronomy and Astrophysics, 29*(3), 274-282.

Sornette, D., Utkin, S., & Saichev, A. (2008). Solution of the nonlinear theory and tests of earthquake recurrence times. *Physical Review E, 77*(6), 066109.

Spiegel, E., & Zahn, J.-P. (1992). The solar tachocline. *Astronomy and Astrophysics, 265*, 106-114.

Srinivasamurthy, Y., Kumar, M. V. A., Sandeep, K. V., VJ, S. M., & Reddy, E. V. (2014). Earth quake prognostication using data mining and curve fitting techniques. *International Journal of Innovative Technology and Research, 2*(5), 1214-1218.

Stenflo, J., & Kosovichev, A. (2012). Bipolar magnetic regions on the Sun: global analysis of the SOHO/MDI data set. *The Astrophysical Journal, 745*(2), 129.

Sukma, I., & Abidin, Z. Z. (2017). Study of seismic activity during the ascending and descending phases of solar activity. *Indian Journal of Physics, 91*(6), 595-606.

Surkov, V., & Hayakawa, M. (2014). *Ultra and extremely low frequency electromagnetic fields*. Berlin, Germany: Springer.

Tenfjord, P., & Østgaard, N. (2013). Energy transfer and flow in the solar wind-magnetosphere-ionosphere system: A new coupling function. *Journal of Geophysical Research: Space Physics, 118*(9), 5659-5672.

Thébault, E., Purucker, M., Whaler, K. A., Langlais, B., & Sabaka, T. J. (2010). The magnetic field of the Earth's lithosphere. *Space Science Reviews, 155*(1-4), 95-127.

Thomas, J. H., & Weiss, N. O. (1992). The theory of sunspots. In J. H. T & N. O. W (Eds.), *Sunspots: theory and observations* (pp. 3-59). Berlin, Germany: Springer.

Tsurutani, B. T., Ho, C. M., Arballo, J. K., Goldstein, B. E., & Balogh, A. (1995). Large amplitude IMF fluctuations in corotating interaction regions: Ulysses at midlatitudes. *Geophysical Research Letters, 22*(23), 3397-3400.

Tyler, R. H., Maus, S., & Lühr, H. (2003). Satellite observations of magnetic fields due to ocean tidal flow. *Science, 299*(5604), 239-241.

Waldmeier, M. (1961). The sunspot-activity in the years 1610-1960. Zurich: Schulthess & Company AG.

Watson, F. T. (2012). *Investigating sunspot and photospheric magnetic field properties using automated solar feature detection.* (Doctoral dissertation), University of Glasgow. Retrieved from http://theses.gla.ac.uk/3429/.

Webb, D. F., & Howard, R. A. (1994). The solar cycle variation of coronal mass ejections and the solar wind mass flux. *Journal of Geophysical Research: Space Physics, 99*(A3), 4201-4220.

Whiteman, C. D. (2000). *Mountain meteorology: fundamentals and applications*. Oxford, United Kingdom: Oxford University Press.

Xiao-Fei, S., Bin-Bin, N., Xu-Dong, G., Chen, Z., Yong, L., Zheng, X., & Zheng-Yu, Z. (2015). A Statistical Analysis of Solar Wind Parameters and Geomagnetic Indices during the Solar Cycle 23. *Chinese Journal of Geophysics, 58*(2), 170-178.

Zakrzhevskaya, N., & Sobolev, G. (2002). On the seismicity effect of magnetic storms. *Izvestiya, Physics of the Solid Earth, 38*(4), 249-261.

LIST OF PUBLICATIONS AND PAPERS PRESENTED

Sukma, I., & Abidin, Z. Z. (2017). Study of seismic activity during the ascending and descending phases of solar activity. *Indian Journal of Physics, 91*(6), 595-606.

Sukma, I., & Abidin, Z. Z. (2014, October). *Is any possible relationship between solar and seismic activities? (CHINA).* Paper presented at the Southeast Asian Young Astronomers Collaboration, University of Malaya, Malaysia.